

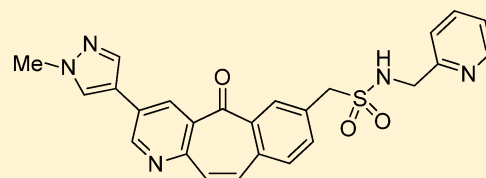
Discovery of 1-[3-(1-Methyl-1*H*-pyrazol-4-yl)-5-oxo-5*H*-benzo[4,5]cyclohepta[1,2-*b*]pyridin-7-yl]-*N*-(pyridin-2-ylmethyl)methanesulfonamide (MK-8033): A Specific *c*-Met/Ron Dual Kinase Inhibitor with Preferential Affinity for the Activated State of *c*-Met

Alan B. Northrup,^{*,†} Matthew H. Katcher,[†] Michael D. Altman,[‡] Melissa Chenard,[§] Matthew H. Daniels,[†] Sujal V. Deshmukh,^{||} Danielle Falcone,[†] David J. Guerin,[†] Harold Hatch,[⊥] Chaomin Li,[†] Wei Lu,[⊥] Bart Lutterbach,[⊥] Timothy J. Allison,[#] Sangita B. Patel,[#] John F. Reilly,[§] Michael Reutershan,[†] Keith W. Rickert,[#] Craig Rosenstein,^{||} Stephen M. Soisson,[#] Alexander A. Szewczak,^{||} Deborah Walker,[×] Kevin Wilson,[†] Jonathan R. Young,[†] Bo-Sheng Pan,[⊥] and Christopher J. Dinsmore[†]

[†]Department of Chemistry, [‡]Department of Chemistry Modeling and Informatics, [§]Department of in Vivo Pharmacology, ^{||}Department of Pharmacokinetics, Pharmacodynamics & Drug Metabolism, [⊥]Department of Oncology, [#]Department of Structural Chemistry, ^{||}Department of in Vitro Pharmacology, [×]Department of Basic Pharmaceutical Sciences, Merck & Co., Inc., 33 Avenue Louis Pasteur, BMB-3, Boston, Massachusetts 02115, United States

Supporting Information

ABSTRACT: This report documents the first example of a specific inhibitor of protein kinases with preferential binding to the activated kinase conformation: 5*H*-benzo[4,5]cyclohepta[1,2-*b*]pyridin-5-one **11r** (MK-8033), a dual *c*-Met/Ron inhibitor under investigation as a treatment for cancer. The design of **11r** was based on the desire to reduce time-dependent inhibition of CYP3A4 (TDI) by members of this structural class. A novel two-step protocol for the synthesis of benzylic sulfonamides was developed to access **11r** and analogues. We provide a rationale for the observed selectivity based on X-ray crystallographic evidence and discuss selectivity trends with additional examples. Importantly, **11r** provides full inhibition of tumor growth in a *c*-Met amplified (GTL-16) subcutaneous tumor xenograft model and may have an advantage over inactive form kinase inhibitors due to equal potency against a panel of oncogenic activating mutations of *c*-Met in contrast to *c*-Met inhibitors without preferential binding to the active kinase conformation.



INTRODUCTION

The discovery and development of protein kinase inhibitors has comprised a substantial proportion of pharmaceutical research over the past decade resulting in several FDA approved drugs. Increasingly, kinase inhibitor discovery efforts have focused on specific inhibitors for a target due to the hypothesis that specificity will result in an improved safety profile versus multikinase inhibitors.¹ Protein kinases can adopt conformations corresponding to different states of phosphorylation and activity. Accordingly, there have been attempts to correlate specificity with compound binding preferences to either active-like or inactive-like protein conformations. To that end, the discovery of type II inhibitors (i.e., those binding to the inactive “DFG-out” conformation first observed with Imatinib in complex with Abl) has fueled a dogma in the field that targeting the inactive conformation with type II inhibitors will demonstrate superior specificity when compared to inhibitors of the activated kinase because the allosteric binding pocket afforded by the DFG-out conformation provides unique opportunities for specificity.² Activating mutations of kinases

are commonly observed in cancer and can also be induced by treatment with type II inhibitors,³ leading to an acute need for agents that target activating mutations in cancer (e.g., Nilotinib for the treatment of Imatinib-resistant chronic myelogenous leukemia).⁴

c-Met and Ron are receptor tyrosine kinase members of the *c*-Met proto-oncogene family and are closely related in structure and function.⁵ *c*-Met is the receptor for hepatocyte growth factor (also known as scatter factor), and Ron is the receptor for macrophage stimulating protein. Abberent expression of *c*-Met and Ron has been correlated with poor prognosis, and activating *c*-Met mutations have been observed in human tumors.⁶ Signaling cross-talk has been observed between the *c*-Met and Ron receptors;⁷ therefore, it may be desirable to inhibit signaling through both receptors for optimal therapeutic benefit. Indeed, concomitant overexpression of

Received: November 2, 2012

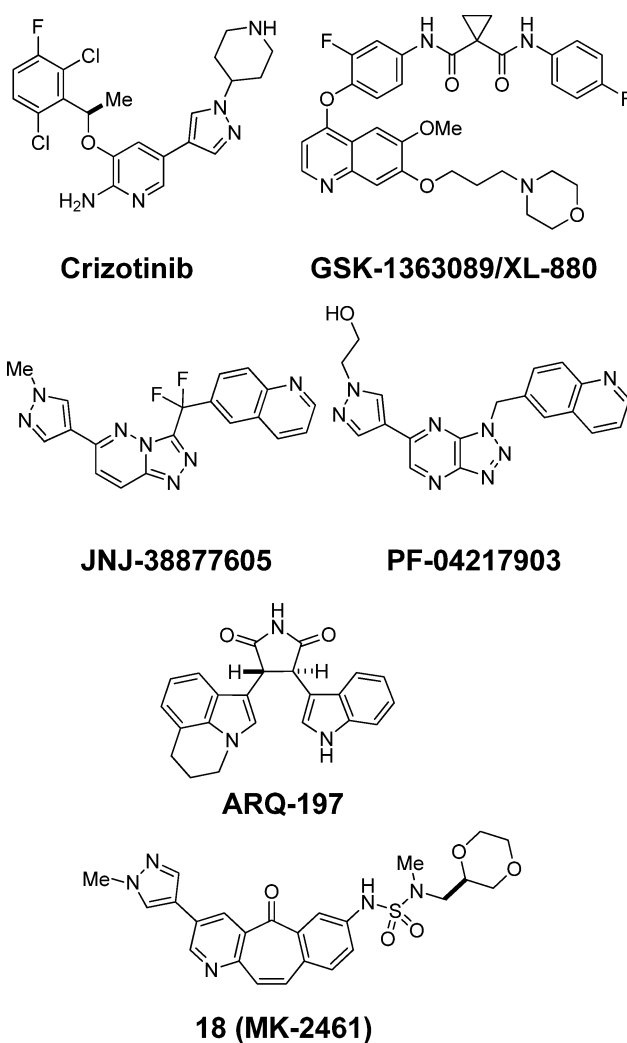
Published: February 4, 2013

both c-Met and Ron are negative prognostic factors in breast⁸ and bladder cancers.⁹

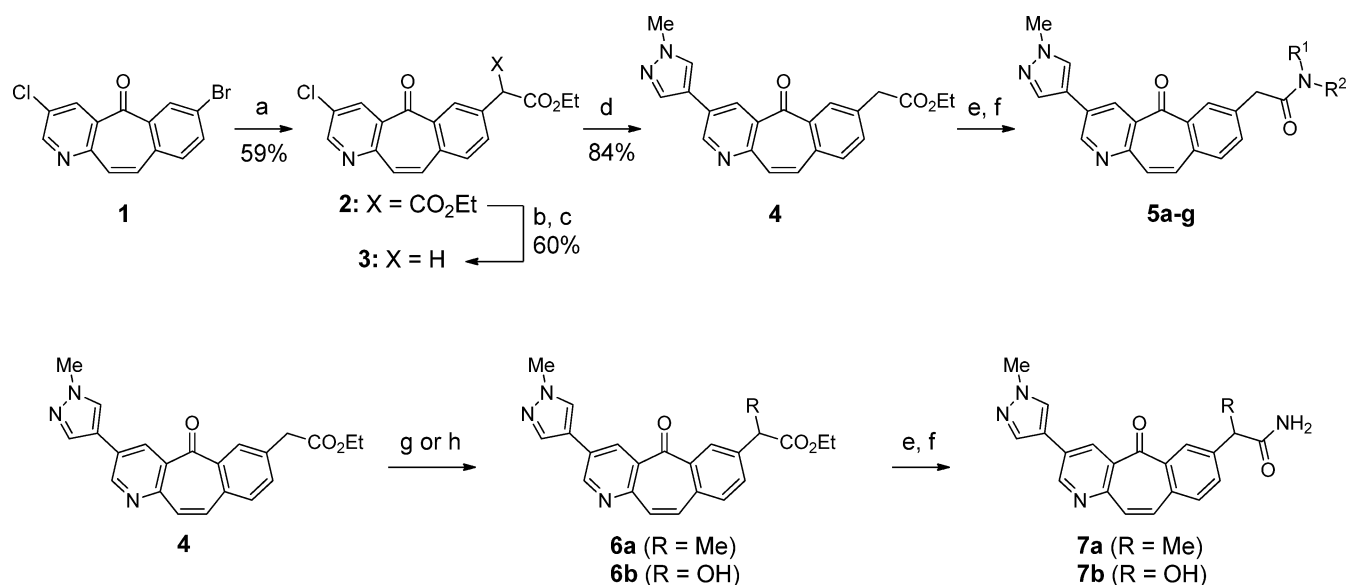
Because of its status as a proto-oncogene, c-Met has attracted significant attention as an anticancer target with several agents in clinical development including one marketed agent, the ALK/c-Met inhibitor Crizotinib.¹⁰ Notably, the type I and type II inhibitors in clinical development are multikinase inhibitors with c-Met inhibition as one of a number of activities (e.g., Crizotinib and GSK-1363089/XL-880,¹¹ respectively). The specific c-Met inhibitors JNJ-38877605¹² (Phase III), EMD-1214063¹³ and PF-04217903¹⁴ (both in phase I clinical studies), respectively, as well as a series of triazolopyridinone inhibitors,¹⁵ are all believed to bind the inactive form of the receptor preferentially although likely not through a classical DFG-out type II binding mode. Interestingly, it has been shown that inactive form binders to c-Met can induce activating resistance mutations in c-Met in cell culture.¹⁶ Additionally, ARQ-197 is reported to be a c-Met inhibitor that was, until recently, in late-stage clinical studies.¹⁷ Our laboratories have previously described the discovery of **18** (MK-2461),¹⁸ a multitargeted c-Met inhibitor that was shown through binding studies and in vitro biochemistry experiments to preferentially bind the activated conformation of c-Met. The current manuscript documents the discovery of **11r** (MK-8033), a specific dual c-Met/Ron inhibitor, demonstrating that both high kinase specificity and also activity against clinically activating mutations can be achieved through targeting the activated kinase conformation.

CHEMISTRY

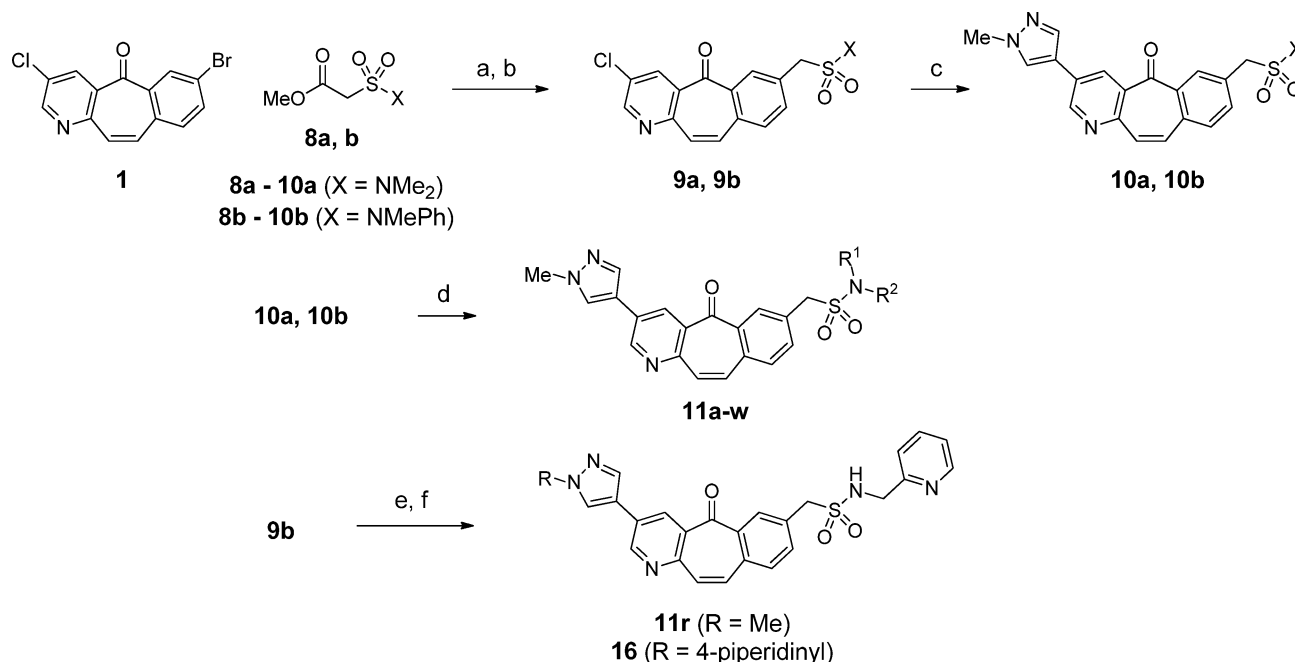
The synthesis of acetamide derivatives is outlined in Scheme 1 from the versatile tricyclic dihalide intermediate **1**. Amides **5a–g** were prepared via arylation of diethylmalonate,¹⁹ followed by decarboxylation, Suzuki–Miyaura coupling and amide formation. Functionalization of the benzylic position was also possible by trapping the corresponding enolate of intermediate



Scheme 1. Synthesis of Acetamide Derivatives^a



^a(a) Pd₂(dba)₃, P(*t*-Bu)₃·HBF₄, dimethylmalonate, K₃PO₄, toluene, 70 °C; (b) 6N HCl, AcOH, 110 °C; (c) SOCl₂, MeOH, reflux; (d) Pd₂(dba)₃, P(*t*-Bu)₃·HBF₄, 1-methyl-4-(4,4,5,5-tetramethyl-1,3,2-dioxaborolan-2-yl)-1H-pyrazole, KF, DMF, 130 °C; (e) 1N NaOH, THF, rt; (f) Et₃N, HATU, amine, CH₂Cl₂, rt; (g) LDA, MeI, THF, -78 °C; (h) LDA, *rac*-(10)-(camphorylsulfonyl)oxaziridine, THF, -78 °C.

Scheme 2. Synthesis of Benzylic Sulfonamide Derivatives^a

^a(a) for **8a**, Pd₂(dba)₃, PPh₃, NaH, dioxane 70 °C; for **8b**, Pd(OAc)₂, P(*t*-Bu)₃·HBF₄, NaOt-Bu, dioxane, 90 °C. (b) 1N NaOH, 50 °C. (c) Pd₂(dba)₃, P(*t*-Bu)₃·HBF₄, 1-methyl-4-(4,4,5,5-tetramethyl-1,3,2-dioxaborolan-2-yl)-1H-pyrazole, KF, DMF, 130 °C. (d) for **9a**, Cs₂CO₃, amine, dioxane, 180 °C; for **9b**, amine, NMP, 190 °C. (e) 2-aminomethylpyridine, NMP, 130–135 °C. (f) for **11r**, Pd₂(dba)₃, PCy₃, lithium 2-hydroxy-4,4,5,5-tetramethyl-2-(1-methyl-1H-pyrazol-4-yl)-1,3,2-dioxaborolan-2-uide hydrate, DMF, 100 °C; for **16**, Pd₂(dba)₃, P(*t*-Bu)₃·HBF₄, KF, *tert*-butyl 4-[4-(4,4,5,5-tetramethyl-1,3,2-dioxaborolan-2-yl)-1H-pyrazol-1-yl]piperidine-1-carboxylate, DMF, 130 °C, then HCl, dioxane.

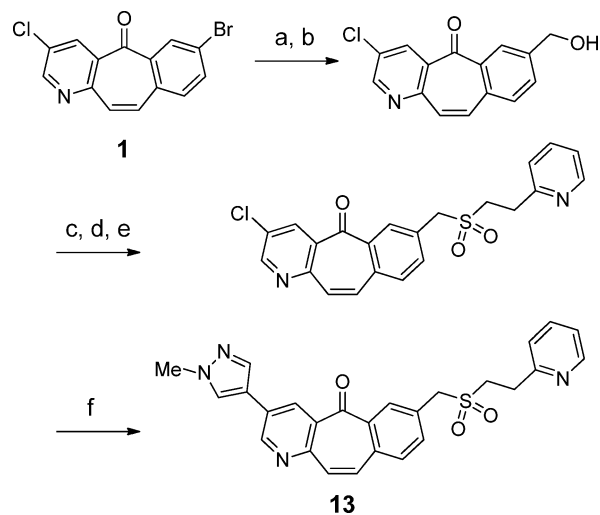
4 with electrophiles to provide esters **6a** and **6b** that were then converted to the corresponding primary amides **7a** and **7b**.

The preparation of benzylic sulfonamide derivatives **11a–y** is outlined in Scheme 2 and required the invention of two new chemical reactions for these structure–activity studies: a palladium-catalyzed coupling of β -sulfamylacetates to afford intermediates **9a** and **9b** and an amine exchange reaction to provide access to a diverse range of products **11a–v** at the final step of the synthesis.²⁰ It was found that exchange reactions of amines with dimethylsulfonamide **10a** required harsh conditions and afforded products **11** in low yield. Replacement of **10a** with intermediate **10b** in amine exchange reactions permitted the use of lower reaction temperatures and provided improved yields of products **11a–w**. The increased reactivity of **10b** is presumably due to the lower pK_a of the *N*-methylaniline leaving group as compared to dimethylamine from **10a**. The use of an exchangeable sulfonamide permitted bidirectional SAR studies that installed either the left-hand aryl or right-hand sulfonamide moiety first in the synthetic operation. For example, compounds **11r** and **16** were prepared via sulfonamide exchange with 2-pyridylmethylamine followed by Suzuki–Miyaura coupling.

Sulfone **13** was prepared as outlined in Scheme 3. Installation of a methanol unit to **1** via cross-coupling and alcohol deprotection was followed by mesylation, displacement with 2-pyridin-2-ylethanethiol, and oxidation to the corresponding sulfone. Suzuki–Miyaura coupling completed the synthesis of **13**.

RESULTS AND DISCUSSION

Prior studies leading to compound **18** established that the tricyclic core binds deeply in the ATP site, adopting a slightly

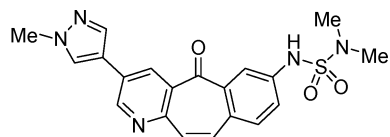
Scheme 3. Synthesis of Sulfone **13**^a

^a(a) Potassium (2-(trimethylsilyl)ethoxy)methyltrifluoroborate Pd(OAc)₂, RuPhos, Cs₂CO₃, 10:1 dioxane/water, 100 °C; (b) BF₃·OEt₂, CH₂Cl₂, 0 °C; (c) MsCl, Et₃N, dioxane, 0 °C; (d) NaH, 2-pyridin-2-ylethanethiol, DMF; (e) MCPBA, CH₂Cl₂; (f) Pd₂(dba)₃, X-Phos, lithium 2-hydroxy-4,4,5,5-tetramethyl-2-(1-methyl-1H-pyrazol-4-yl)-1,3,2-dioxaborolan-2-uide hydrate, DMF, 150 °C.

benzyl geometry, with the pyridine nitrogen making a hydrogen bond interaction with the hinge backbone (Figure 2E). Only substitution at the 3 and 7 positions of the tricyclic core were compatible with achieving the desired potency, as these unburied positions extend toward solvent and the catalytic residues, respectively.¹⁸ To improve on **18**, we focused on the simpler *N,N*-dimethylsulfamide analogue **12**, which was an

intriguing lead for further optimization based on its desirable properties (Table 1). While **12** displayed favorable potency

Table 1. Properties of Compound **12**



12

Potency

c-Met IC ₅₀ (nM)	4
Ron IC ₅₀ (nM)	7
GTL-16 pY ¹³⁴⁹ Cell IC ₅₀ (nM)	80
GTL-16 Proliferation IC ₅₀ (nM)	2,300

TDI of CYP3A4^a

%CYP3A4 Activity Lost @ 50 μM	52%
%CYP3A4 Activity Lost @ 10 μM	30%

Pharmacokinetics:

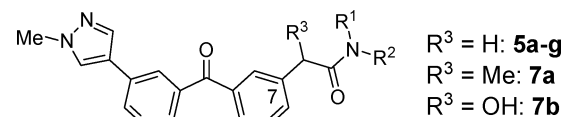
Species	Rat	Dog
Cl _p (mL/min/kg)	40	57
V _d (L/kg)	2.5	3.5
t _{1/2} (hr)	0.7	0.8
%F	24%	16%

^aCYP3A4 enzyme and inhibitor are preincubated for 30 min at the indicated concentration and the enzyme activity is compared to a zero minute incubation control with the same inhibitor to calculate the percentage of lost activity via preincubation. See Experimental Section for details.

(enzymatic and cellular), pharmacokinetic parameters, and lacked appreciable inhibition of the hERG ion channel, dimethylsulfamide **12** was found to be a potent time-dependent inhibitor of CYP3A4 (TDI) and also inhibited various kinase off-targets beyond c-Met and Ron (see Supporting Information). It is well-known that reversible or time-dependent CYP inhibitors can inhibit the metabolism of common anticancer agents, resulting in increased clinical AUCs and potentially toxicity given the narrow therapeutic index displayed by many oncology drugs.²¹ As the standard of care for most oncology patients involves combinatorial therapy, it is desirable for new agents not to perpetrate drug–drug interactions; therefore, minimizing TDI was a major consideration for molecular design.

While metabolite ID experiments were unable to pinpoint the site of oxidation on the tricyclic core structure of **12**, it was hypothesized the electron-rich aniline substructure present in **12** may be responsible for the observed TDI given the well-known propensity for bioactivation of anilines.²² While the initial intent was to prepare sulfonamide **11c** as a direct comparator to sulfamide **12**, initial attempts at the synthesis of **11c** were unsuccessful and a series of C-7 substituted tricyclic acetamides were evaluated to test the hypothesis that sulfamide replacements would alleviate the TDI issue (Table 2). Unfortunately, a >100-fold loss in potency was observed for dimethylamide **5c** vs dimethylsulfamide **12** as well as for the direct analogues of **18** and **11r**: **5f** and **5g**, respectively. A partial recovery of the lost potency was noted with the introduction of

Table 2. Potency of C-7 Acetamides

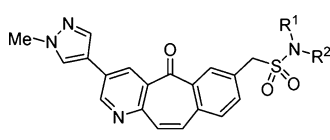


	NR ¹ R ²	c-Met IC ₅₀ (nM)	GTL-16 pY1349 IC ₅₀ (nM)
5a	NH ₂	60	861
5b	NHMe	1,888	ND
5c	NMe ₂	1,157	ND
5d	NHPh	2,691	ND
5e	NHBn	94	2,293
5f		3,191	ND
5g		1,368	ND
7a	NH ₂	70	912
7b	NH ₂	32	403

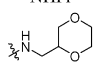
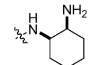
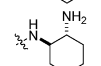
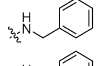
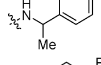
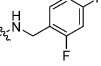
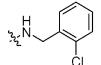
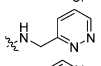
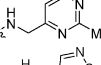
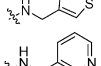
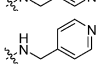
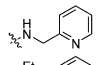
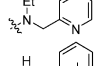
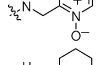
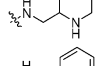
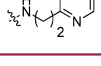
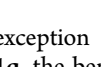
primary amides **5a**, **7a**, and **7b** but not amides **5b**, **5c**, and **5e**. While encouraging results in cellular biochemical potency were achieved for compound **7b**, attempts at further potency optimization were not successful. As the primary hypothesis for preparing compounds **5** and **7** was to understand whether C-7 carbon analogues of **12** would remove the TDI liability, compounds **5a** and **5g** were selected for further evaluation.

To monitor the risk of TDI of CYP3A4, a screening assay was employed that measures the activity of CYP3A4 to metabolize testosterone with either 0 or 30 min of preincubation of CYP3A4 with the test article. The percentage of CYP3A4 activity lost due to preincubation was then calculated and reported as the primary end point for the assay.²³ On the basis of kinetic considerations, assay variability and internal experience translating the screening results to more definitive kinetic experiments, results with <30% CYP3A4 activity lost in this screening assay are considered to have a low risk of demonstrating significant TDI of CYP3A4, whereas compounds showing >50% lost are likely to demonstrate TDI of CYP3A4. Gratifyingly, both **5a** and **5g** demonstrated <10% CYP3A4 activity lost, providing support for the hypothesis that C-7 carbon-substituted analogues of **12** may reduce the potential for TDI of CYP3A4.

With the aim of maintaining a favorable CYP inhibition profile while improving potency relative to the acetamides **5** and **7**, a series of benzylic sulfonamides were investigated (Table 3) following the invention of two new chemical reactions: the palladium-catalyzed coupling of β-sulfamylacetates and an amine exchange reaction. Similar to the acetamides above, benzylic sulfonamides **11a–v** were typically not time-dependent inhibitors of CYP3A4, except for aniline derivative

Table 3. Potency and CYP Inhibition of Diverse C-7 Benzylic Sulfonamides


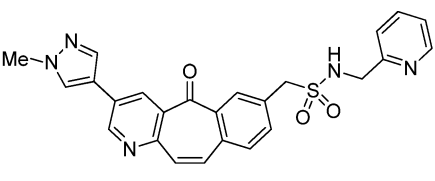
11a-y

	NR ¹ R ²	c-Met IC ₅₀ nM	CYP3A4 %Inh. @10 μM	TDI %Lost 10 μM
11a	NH ₂	98	0	26
11b	NHMe	163	0	35
11c	NMe ₂	2,294	0	6
11d	NHPr	42	21	15
11e		45	0	35
11f		53	27	20
11g		14	30	30
11h	NHPh	33	28	50
11i		11	ND	ND
11j		52	ND	ND
11k		6	42	17
11l		5	17	0
11m		1	23	14
11n		3	22	5
11o		3	67	13
11p		8	30	0
11q		3	97	ND
11r		1	31	16
11s		4,950	ND	ND
11t		2	24	0
11u		67	29	1
11v		55	14	9

11h. With the exception of isothiazole **11o** and 4-aminomethylpyridine **11q**, the benzylic sulfonamides displayed <50% reversible inhibition of CYP3A4 at 10 μM. The benzylic sulfonamides, in contrast to acetamides **5** and **7**, tolerated a broad range of amine substituents while maintaining favorable potency. Simple primary and secondary alkyl sulfonamides were moderately potent (e.g., **11a**, **11b**, **11d** c-Met IC₅₀ = 42–163 nM), whereas tertiary sulfonamides **11c** and **11s** were substantially less potent (c-Met IC₅₀ = 2294, 4950 nM, respectively), similar to modestly improved potency observed with the introduction of either polar (e.g., **11e** c-Met IC₅₀ = 45

nM) or cyclic alkyl substituents (e.g., **11f**, **11g** c-Met IC₅₀ = 53, 14 nM, respectively). Significant increases in potency, in contrast, were observed with benzylamines (e.g., **11i,k,l** c-Met IC₅₀ = 5–11 nM) and, in particular, heterocyclic methylamine analogues (e.g., **11m–r** c-Met IC₅₀ = 1–8 nM). Aminomethylbenzene derivative **11j** demonstrated substitution α to the sulfonamide nitrogen affords diminished potency (c-Met IC₅₀ = 52 nM). Sulfonamide N-alkylation provided >1000× loss in potency, supporting a critical role for a C-7 hydrogen-bond donor for maintaining c-Met potency (cf. **11r** and **11s**). The overall profile of 2-aminomethylpyridine derivative **11r** warranted further exploration of the SAR. While pyridine N-oxidation provides equivalent potency (**11t** c-Met IC₅₀ = 2 nM), saturated or homologated analogues are less potent (**11u**, **11v** c-Met IC₅₀ = 67, 55 nM, respectively) but still retain the favorable CYP inhibition profile of **11r**.

On the basis of a superior in vivo PK profile vs other analogues with favorable potency and minimal CYP inhibition (e.g., **11m**, **11n**, **11t**), aminomethylpyridine derivative **11r** was selected for further profiling (Table 4). Evaluation of CYP3A4

Table 4. Properties of 11r


11r

Potency		
c-Met IC ₅₀ (nM)	1	
Ron IC ₅₀ (nM)	7	
GTL-16 pY ¹³⁴⁹ Cell IC ₅₀ (nM)	29	
GTL-16 Proliferation IC ₅₀ (nM)	580	
Cytochrome P450 Inhibition		
CYP3A4 IC ₅₀ (nM)	11,580	
CYP2C9 IC ₅₀ (nM)	14,730	
CYP2D6 IC ₅₀ (nM)	46,170	
CYP3A4 TDI	none detected up to 100 μM	
Pharmacokinetics:		
Species	Rat	Dog
Cl _p (mL/min/kg)	20	3.1
V _d (L/kg)	0.4	0.7
t _{1/2} (hr)	0.8	3.1
F%	35%	33%

inhibition kinetics confirmed the screening data in Table 3 that **11r** is not a time-dependent inhibitor of CYP3A4 up to a test concentration of 100 μM. Compound **11r** is a weak inhibitor of cytochrome P450s at high μM concentrations (IC₅₀s > 11 μM). Taken together, those data indicate **11r** has a low risk of perpetrating CYP-mediated drug–drug interactions. Additionally, **11r** exhibits low to moderate clearance in rats and dogs and also favorable bioavailability in both species. **11r** potently inhibited c-Met/HGF-dependent cellular phenotypes in vitro. These include phosphorylation of Y1349 of c-Met in the c-Met-dependent gastric cancer cell line GTL-16 (IC₅₀ = 0.03 μM) and proliferation of the same cell line (IC₅₀ = 0.58 μM).

On the basis of the structural homology of **11r** to **18**, we reasoned that **11r** may also preferentially bind to and inhibit the catalytic activity of activated c-Met kinase. Such a mode of action is further supported by a BIAcore-based direct binding assay showing that **11r** binds 3-fold more tightly to phosphorylated c-Met kinase domain ($K_d = 3.2$ nM) than to its unphosphorylated counterpart ($K_d = 10.4$ nM). Significantly, **11r** potently inhibits kinase activity of three oncogenic c-Met activation loop mutants, Y1230C, Y1230H, and Y1235D (IC_{50} s ranging from 0.6 to 1 nM at 50 μ M ATP, Table 5) in addition to other c-Met activating mutants N1100Y and M1250T.

Table 5. In Vitro Inhibitory Effect of 11r on Wild Type and Mutant c-Met Kinases

enzyme	mean IC_{50} (nM)
WT c-Met	1.3
c-Met(N1100Y)	2.0
c-Met(Y1230C)	1.0
c-Met(Y1230H)	0.6
c-Met(Y1235D)	0.6
c-Met(M1250T)	1.2

To our surprise, **11r** is a highly specific c-Met/Ron dual inhibitor. Compound **11r** was tested at 1 μ M using a panel of 221 kinases. Only two kinases, c-Met and Ron, were inhibited by more than 90% and merely four other kinases (Fes, FGFR3, Flt4, and Mer) were inhibited by more than 50%, with the inhibition ranging from 60 to 70%. Follow-up titration experiments demonstrated **11r** is >100-fold selective relative to Ron and c-Met inhibition versus the measured kinome (see Supporting Information).

Because of the exquisite dual c-Met/Ron specificity of **11r** unlike the structurally related **18**, several analogues were assessed in broad kinase panels to help understand the basis for kinase selectivity (Table 6). Surprisingly, minor modifications to the structure of **11r** led to dramatic loss of either potency or selectivity. For example, replacement of the **11r** sulfonamide with a sulfone, sulfamide, or amide in compounds **13**, **14**,¹⁸ and **5g** lost 10- to >100-fold potency and engendered similar off-targets as **18**. Removal of the aminomethylpyridine moiety to afford compound **11a** also resulted in lost potency and selectivity. Homologation of acetamide **5g** to propionamide **15**,²⁵ however, was successful in both improving the potency 10-fold and also achieving a c-Met specific profile, albeit with ~80-fold reduced potency relative to **11r**.

It was hoped that an X-ray cocrystal structure of **11r** with c-Met could provide valuable insights into explaining the origin of kinase selectivity for **11r**. While attempts to crystallize **11r** with c-Met failed, the X-ray crystal structure of **16** bound to the doubly phosphorylated form of c-Met (activation loop sites pY1234 and pY1235) was determined to 1.99 Å resolution (see Supporting Information Table S9). Compound **16** has comparable kinase selectivity to **11r** and differs from compound **11r** only due to the nature of the pyrazole substituent, which is solvent directed. Similar to what our laboratories have reported for sulfamide **17**¹⁸ and amide **15**²⁵ bound to activated c-Met (Figure 1), sulfonamide **16** binds deeply in the ATP-site, adopting a slightly bent geometry while making a key hydrogen bonding interaction to the hinge region (Met-1160) via the pyridyl nitrogen of the tricyclic ring system (Figure 2A,B,E). However, unlike **17**, compound **16** does not make a key hydrogen bond to the carboxylate side chain of Asp-1222, a

Table 6. Potency and Selectivity of 11r and Analogues

R¹ = Me (**5g**, **11a-w**, **13-14**)
R¹ = 4-piperidinyl (**15**, **16**)

R ²	c-Met IC_{50} nM	Kinases >50% Inh. @ 1 μ M /Tested	Selected Top Kinase Activities ^a
	2	23/209	Met, Ron, Flt, Mer, FGFR, KDR, Aur
	1	3/221	Met, Ron
	190	4/96	Met, FGFR, Aur, KDR, Flt
	10	20/144	Met, Mer, Aur, KDR, Flt, FGFR, Ron
	1,368	24/101 ^b	Met, Aur, KDR, Abl, Flt, FGFR
	98	8/96	Met, MARK1, Aur, KDR, FGFR
	45	8/96	Met, MARK1, Aur, KDR, FGFR
	67	8/96	Met, MARK1, Aur, KDR, FGFR
	8	1/144 ^c	Met, Ron
	85	1/144	Met, RSK3, Aur
	1	1/96	Met

^aSee Supporting Information for complete selectivity profiles. ^b10 μ M test concentration. ^c0.1 μ M test concentration.

residue involved in catalysis that is conserved throughout the kinome (Figures 2B,E). On the basis of the SAR around **18**, this interaction is likely responsible for a significant portion of its potency.¹⁸ This suggests that the interactions made by the sulfonamide region of **11r** and **16** likely provide a comparable enhancement of potency but in a c-Met/Ron selective manner. The sulfonamide NH of **16** makes a hydrogen bond to the side chain carbonyl of Asn-1209, a conserved residue among **18** off-targets, which in turn directs the pyridine ring into a small pocket formed by the backbone of the glycine-rich loop (residues 1086–1088) and the side chains of His-1088 and Arg-1208 (Figures 2B,C). The pyridine ring forms an edge-face interaction with His-1088 and a face-face π -stacking

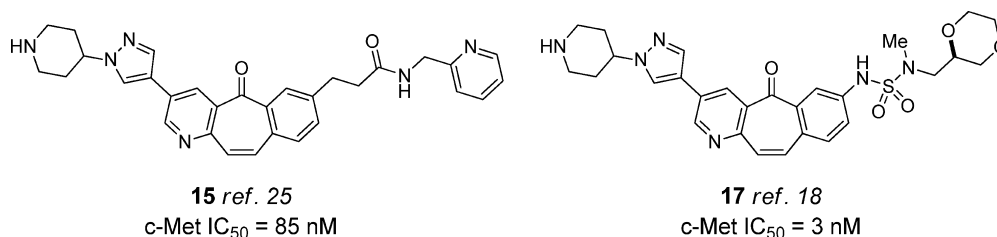


Figure 1. c-Met ligands 15 and 17.

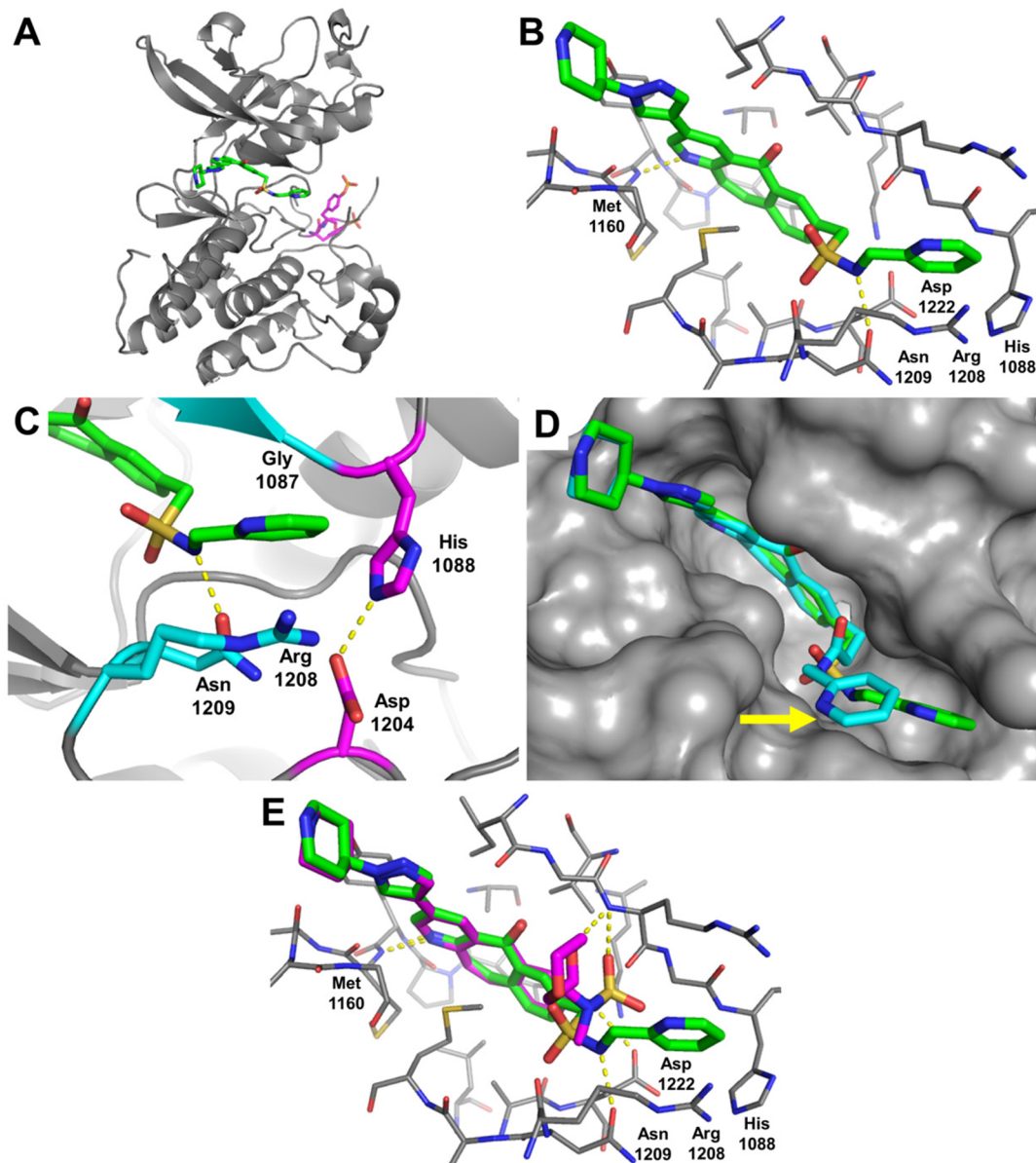


Figure 2. (A) Ribbon cartoon image of the X-ray crystal structure of **16** (green) bound to activated c-Met kinase domain (gray). Phosphotyrosines pY1234 and pY1235 (magenta) part of the activation loop are also highlighted. (B) Binding pose of **16** in the ATP binding pocket. (C) Close-up view of the interactions of **16** with c-Met. (D) Overlay of the structures of **15** (cyan)²⁵ and **16** (green) bound to activated c-Met. The yellow arrow highlights the different disposition of the pyridymethylamine fragment between the two structures. (E) Overlay of the structures of **17** (magenta)¹⁸ and **16** (green) bound to activated c-Met.

interaction with Arg-1208, which is recruited by the inhibitor. To form this pocket, the glycine-rich loop closes down on **16** as compared to the structure of c-Met bound to **17**, such that His-1088 makes an apparent salt bridge with Asp-1204 in the C-terminal lobe (Figure 2C). It is interesting to note that His-

1088 is a unique residue to c-Met and Ron as compared within the off-target kinases of **18**. To probe whether the direct aryl-aryl interactions between inhibitors and His-1088/Arg-1208 were important for selectivity, saturated derivatives such as **11e**, **11u**, and **11w** were prepared. Although some of these

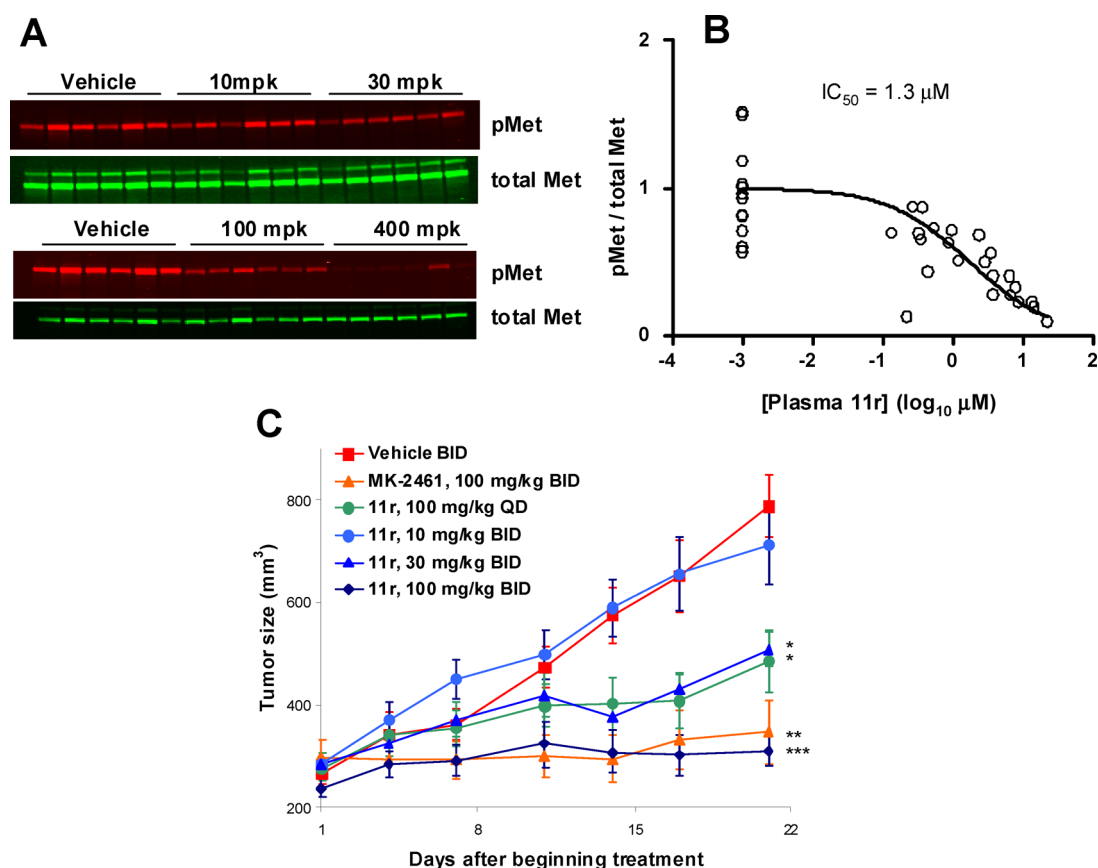


Figure 3. GTL-16 tumor xenograft PK/PD and efficacy of **11r**. (A) Inhibition by **11r** of c-Met (Y1349) phosphorylation in GTL-16 tumors. The tumor bearing mice were given a single oral dose of 10, 30, 100, or 400 mg/kg of **11r** and euthanized 1 h after dosing. The extent of c-Met (Y1349) phosphorylation in the tumors was determined by quantitative Western blotting. Shown are representative images of phospho-c-Met (Y1349) and total c-Met blots. (B) The relationship between the phospho-c-Met (Y1349) levels of all individual tumors and the corresponding host plasma total **11r** concentrations. (C) The effects of orally administered **11r** on the growth of GTL-16 tumor. Asterisks indicate statistically significant difference from vehicle-treated group based on two way repeated measures ANOVA (* $P < 0.05$, ** $P = 0.011$, *** $P < 0.01$).

compounds exhibited reduced potency against c-Met, their selectivity profiles remained c-Met/Ron selective (Table 6). This led us to the alternative hypothesis that perhaps filling the pocket created by a more closed glycine-rich loop conformation (potentially mediated by His-1088) was important for selectivity. This hypothesis was partially challenged by the discovery of selective c-Met/Ron compounds such as **15**. In the previously reported structure of **15** bound to c-Met,²⁵ the pyridyl amide region does not enter this pocket but is instead directed toward solvent (Figure 2D). However, the c-Met glycine-rich loop does adopt the same closed conformation as observed with **16** even though **15** does not occupy this region. Therefore, the induction of this conformation, potentially mediated by His-1088, could be a structural mechanism for c-Met/Ron selectivity although these results highlight the difficulty in generally ascribing the selectivity trends in Table 6 to specific structural features.

The c-Met amplified cell line GTL-16 expresses a highly activated c-Met kinase and is sensitive to c-Met small molecule inhibitors.²⁴ **11r** potently inhibited GTL-16 proliferation with an IC_{50} of 582 ± 30 nM. By contrast, the HCT116 cell line, which does not harbor basal c-Met activation, was not inhibited by **11r** ($IC_{50} > 10000$ nM). Further analysis of larger cell panels confirmed that **11r** selectively inhibited growth in c-Met amplified cell lines.²⁶

To determine plasma levels required to inhibit Met phosphorylation, **11r** was orally dosed in GTL-16 tumor xenograft bearing mice. Mice were euthanized 1 h after dosing and tested for p-Met(Y1349) in tumors and **11r** concentrations in plasma. At 100 mg/kg, essentially complete inhibition of p-Met (Y1349) was achieved. An in vivo IC_{50} of $1.3 \mu\text{M}$ was deduced from the relationship between plasma **11r** level and Met pY1349 (Figure 3B). This IC_{50} is a 45-fold shift from the in vitro IC_{50} (<12 nM) in 10% fetal bovine serum, most likely due to compound binding to plasma proteins in vivo. An IC_{50} of $1.7 \mu\text{M}$ was also obtained when samples were collected after an 8 h time point (data not shown).

Antitumor activity of **11r** was evaluated in human GTL-16 c-Met amplified gastric tumor xenografts in CD1-nude mice. Treatment with escalating doses of **11r** (bid, po) for 21 days led to antitumor efficacies in a dose-dependent manner. Dosing at 3, 10, 30, and 100 mg/kg resulted in 22, 18, 57, and 86% tumor growth inhibition, respectively, relative to tumors from vehicle-treated mice (Figure 3, and Supporting Information Table S10). We also observed significant tumor inhibition with 100 mg/kg **11r** with once daily dosing. Efficacy at 100 mg/kg bid **11r** was comparable to that of the previously described multitargeted c-Met inhibitor **18** also dosed at 100 mg/kg/bid. Finally, treatment with **11r** had no effect on body weight or animal body weight relative to control animals. Analysis of the time course of exposure in the GTL-16 xenograft efficacy

experiment (see Supporting Information) relative to the ex vivo determined p-Met(Y1349) IC₅₀ is supportive of the notion that plasma concentrations exceeding IC₅₀ for 16 h per day is required for maximal efficacy.

CONCLUSIONS

Replacement of the sulfamide substructure on the 5H-benzo[4,5]cyclohepta[1,2-*b*]pyridin-5-ones scaffold present in **12** with a range of sulfonamides provided compounds with reduced potential to perpetrate drug–drug interactions via TDI of CYP3A4 while retaining preferential binding to the activated kinase conformation. **11r** is the first example of a specific kinase inhibitor with preferential binding to the activated kinase conformation; however, the structural basis of its specificity is not fully established as close analogues such as **14** do not retain the high degree of specificity. **11r** is also unique among clinical c-Met inhibitors as it also inhibits Ron with similar potency to c-Met. Importantly, **11r** provides full inhibition of tumor growth in a c-Met amplified (GTL-16) subcutaneous tumor xenograft model and may have an advantage over inactive form kinase inhibitors due to equal potency against a panel of oncogenic activating mutations of c-Met in contrast to results reported with c-Met inhibitors lacking preferential binding to the active kinase conformation.

EXPERIMENTAL SECTION

Chemistry. Commercial reagents were obtained from reputable suppliers and used as received. All solvents were purchased in septum-sealed bottles stored under an inert atmosphere. All reactions were sealed with septa through which an argon atmosphere was introduced unless otherwise noted. Liquid reagents and solvents were transferred under a positive pressure of nitrogen via syringe. Reactions were conducted in microwave vials or round-bottomed flasks containing Teflon-coated magnetic stir bars. Microwave reactions were performed with a Biotage Initiator series microwave (fixed hold time setting; reaction temperatures monitored by the internal infrared sensor).

Reactions were monitored by thin layer chromatography (TLC) on precoated TLC glass plates (silica gel 60 F254, 250 μm thickness) or by LC-MS (30 mm × 2 mm 2 μm column + guard; 2 mL injection; 3–98% MeCN/water + 0.05% TFA gradient over 2.3 min; 0.9 mL/min flow; APCI; positive ion mode; UV detection at 254 nm). Visualization of the developed TLC chromatogram was performed by fluorescence quenching. Flash chromatography was performed on an automated purification system using prepacked silica gel columns. ¹H and ¹³C NMR were recorded on a 500 MHz Varian spectrometer; chemical shifts (δ) are reported relative to residual protio solvent signals. Data for NMR spectra are reported as follows: chemical shift (δ ppm), multiplicity (s = singlet, brs = broad singlet, d = doublet, t = triplet, q = quartet, dd = doublet of doublets, m = multiplet), coupling constant (Hz), integration.

All compounds reported are of at least 95% purity, as judged by LCAP (150 mm × 4.6 mm ID, 5 μm column; 5 μL injection; 10–100% MeCN/H₂O + 0.05% TFA gradient over 6.75 min; 1 mL/min flow; ESI; positive ion mode; UV detection at 254 nm).

Diethyl (3-Chloro-5-oxo-5H-benzo[4,5]cyclohepta[1,2-*b*]pyridin-7-yl)propanedioate (2). A flask was charged with tricyclic dihalide **1** (500 mg, 1.56 mmol), Pd₂(dba)₃ (57 mg, 0.062 mmol), tri-*tert*-butylphosphine HBF₄ salt (36 mg, 0.13 mmol), diethyl malonate (0.30 mL, 2.0 mmol), and potassium phosphate (1010 mg, 4.77 mmol), placed under an inert atmosphere, and then toluene (7.8 mL) was added. The reaction mixture was heated to 70 °C with stirring overnight, then cooled to room temperature and filtered through a plug of silica gel, washing with dichloromethane. The filtrate was concentrated under reduced pressure, and the residue was purified by column chromatography on silica gel eluting with EtOAc/hexanes to afford the title compound (369 mg, 0.924 mmol, 59% yield) as an orange oil that slowly began to crystallize upon standing. ¹H NMR

(500 MHz, DMSO-*d*₆) δ 8.98 (d, *J* = 2.0 Hz, 1H), 8.46 (d, *J* = 2.0 Hz, 1H), 8.18 (d, *J* = 1.5 Hz, 1H), 7.82 (m, 2H), 7.47 (d, *J* = 10.5 Hz, 1H), 7.32 (d, *J* = 10.0 Hz, 1H), 5.28 (s, 1H), 4.15 (m, 4H), 1.16 (m, 6H). MS (APCI) calcd for C₂₁H₁₉ClNO₅ [M + H]⁺, 400.1; found, 400.1.

Ethyl [3-(1-Methyl-1H-pyrazol-4-yl)-5-oxo-5H-benzo[4,5]-cyclohepta[1,2-*b*]pyridin-7-yl]acetate (4). Step 1: Diethyl (3-chloro-5-oxo-5H-benzo[4,5]cyclohepta[1,2-*b*]pyridin-7-yl)propanedioate (4.12 g, 10.3 mmol) was dissolved in 6N HCl (25.0 mL, 150 mmol) and AcOH (25.0 mL) and then heated to 110 °C. After 2 h, the reaction mixture was concentrated under reduced pressure. The residual yellow solid (3.09 g, 10.3 mmol) was suspended in ethanol (51.6 mL), and then SOCl₂ (1.88 mL, 25.8 mmol) was added dropwise with stirring. The resulting solution was then heated to reflux for 2 h and then cooled to room temperature. Aqueous sodium hydrogen carbonate (saturated, 500 mL) was cautiously added, and the resulting mixture was extracted with ethyl acetate (3 × 150 mL). The combined organics were dried over anhydrous Na₂SO₄, filtered, and concentrated under reduced pressure. The residue was purified by column chromatography on silica gel eluting with EtOAc/hexanes to afford ethyl (3-chloro-5-oxo-5H-benzo[4,5]cyclohepta[1,2-*b*]pyridin-7-yl)acetate (2.03 g, 6.19 mmol, 60% yield) as a white solid. MS (APCI) calcd for C₁₈H₁₅ClNO₃ [M + H]⁺, 328.1; found, 328.0.

Step 2: Ethyl (3-chloro-5-oxo-5H-benzo[4,5]cyclohepta[1,2-*b*]pyridin-7-yl)acetate (2.03 g, 6.19 mmol), 1-methyl-4-(4,4,5,5-tetramethyl-1,3,2-dioxaborolan-2-yl)-1H-pyrazole (1.55 g, 7.43 mmol), tri-*tert*-butylphosphonium tetrafluoroborate (162 mg, 0.557 mmol), Pd₂(dba)₃ (227 mg, 0.248 mmol), and potassium fluoride (1.19 g, 20.4 mmol) were combined in a vial and then placed under a nitrogen atmosphere. DMF (61.9 mL) was added, and the resulting suspension was heated to 130 °C and left to stir for 1 h. The reaction mixture was then poured into aqueous sodium hydrogen carbonate (500 mL) and extracted with dichloromethane (5 × 100 mL). The combined organics were dried over anhydrous Na₂SO₄, filtered, and concentrated under reduced pressure. The residue was purified by column chromatography on silica gel eluting with EtOAc/hexanes to ethyl acetate + 10% methanol to afford the title compound (1.95 g, 5.23 mmol, 84% yield) as an orange solid. ¹H NMR (500 MHz, DMSO-*d*₆) δ 9.20 (d, *J* = 2.0 Hz, 1H), 8.53 (d, *J* = 1.5 Hz, 1H), 8.46 (s, 1H), 8.13 (s, 1H), 8.04 (d, 1.5 Hz, 1H), 7.75 (d, *J* = 7.0 Hz, 1H), 7.69 (dd, *J* = 7.0, 1.5 Hz, 1H), 7.38 (d, *J* = 10.5 Hz, 1H), 7.29 (d, *J* = 10.0 Hz, 1H), 4.08 (q, *J* = 6.0 Hz, 2H), 3.88 (s, 3H), 3.87 (s, 2H), 1.17 (t, *J* = 6 Hz, 3H). MS (APCI) calcd for C₂₂H₂₀N₃O₃ [M + H]⁺, 374.1; found, 374.2.

[3-(1-Methyl-1H-pyrazol-4-yl)-5-oxo-5H-benzo[4,5]-cyclohepta[1,2-*b*]pyridin-7-yl]acetic Acid. Ethyl [3-(1-methyl-1H-pyrazol-4-yl)-5-oxo-5H-benzo[4,5]cyclohepta[1,2-*b*]pyridin-7-yl]acetate (1.00 g, 2.68 mmol) was suspended in THF (10.7 mL) and 1N NaOH (5.36 mL, 5.36 mmol) with stirring. After 90 min, the reaction was neutralized with 1N HCl (5.36 mL) to form a yellow solution that was poured into brine (50 mL). A yellow precipitate was formed, collected via filtration, and dried under reduced pressure. The filtrate was extracted with ethyl acetate, dried over anhydrous Na₂SO₄, filtered, and concentrated under reduced pressure. The residue was combined with the dried filter cake to afford the title compound (867 mg, 2.51 mmol, 94% yield) as a yellow solid. ¹H NMR (500 MHz, DMSO-*d*₆) δ 12.5 (br s, 1H), 9.20 (d, *J* = 2.0 Hz, 1H), 8.53 (d, *J* = 2.0 Hz, 1H), 8.46 (s, 1H), 8.13 (s, 1H), 8.03 (d, 1.5 Hz, 1H), 7.74 (d, *J* = 6.5 Hz, 1H), 7.69 (dd, *J* = 7.0, 2.0 Hz, 1H), 7.38 (d, *J* = 10.0 Hz, 1H), 7.29 (d, *J* = 10.5 Hz, 1H), 3.88 (s, 3H), 3.78 (s, 2H). MS (APCI) calcd for C₂₀H₁₆N₃O₃ [M + H]⁺, 346.1; found, 346.1.

2-[3-(1-Methyl-1H-pyrazol-4-yl)-5-oxo-5H-benzo[4,5]-cyclohepta[1,2-*b*]pyridin-7-yl]acetamide (5a). Triethylamine (101 μL, 0.724 mmol) and HATU (55 mg, 0.15 mmol) were added, followed by 2 M ammonia in isopropyl alcohol (145 μL, 0.290 mmol) to a suspension of [3-(1-methyl-1H-pyrazol-4-yl)-5-oxo-5H-benzo[4,5]cyclohepta[1,2-*b*]pyridin-7-yl]acetic acid (50 mg, 0.145 mmol) in dichloromethane (1.5 mL). After 3 h, the reaction was concentrated under reduced pressure and then the residue was purified by preparative HPLC (reverse phase (C-18), eluting with acetonitrile/water + 0.1% TFA) to afford the title compound (34 mg, 0.098 mmol,

68% yield) as a yellow solid. ^1H NMR (500 MHz, $\text{DMSO}-d_6$) δ 9.19 (d, $J = 1.5$ Hz, 1H), 8.52 (d, $J = 1.5$ Hz, 1H), 8.45 (s, 1H), 8.12 (s, 1H), 8.03 (d, 1.0 Hz, 1H), 7.72 (d, $J = 6.5$ Hz, 1H), 7.68 (dd, $J = 6.5$, 1.5 Hz, 1H), 7.58 (s, 1H), 7.37 (d, $J = 10.0$ Hz, 1H), 7.28 (d, $J = 10.0$ Hz, 1H), 6.97 (s, 1H), 3.88 (s, 3H), 3.55 (s, 2H). MS (APCI) calcd for $\text{C}_{20}\text{H}_{17}\text{N}_4\text{O}_2$ $[\text{M} + \text{H}]^+$, 345.1; found, 345.2. **5b–g** were prepared according to the protocol employed for the synthesis of **5a**.

Ethyl 2-[3-(1-methyl-1H-pyrazol-4-yl)-5-oxo-5H-benzo[4,5]cyclohepta[1,2-b]pyridin-7-yl]propanoate (6a). Ethyl [3-(1-methyl-1H-pyrazol-4-yl)-5-oxo-5H-benzo[4,5]cyclohepta[1,2-b]pyridin-7-yl]acetate (250 mg, 0.670 mmol) was dissolved in THF (6.7 mL) and then cooled to -78 °C. LDA (0.670 mL, 1.34 mmol) was added dropwise, and the resulting solution was stirred at -78 °C for 30 min. Then, methyl iodide (0.084 mL, 1.4 mmol) was added dropwise. After 15 min, the reaction mixture was neutralized with 1 M HCl (1.5 mL) and partitioned between saturated aqueous sodium hydrogen carbonate (100 mL) and dichloromethane (50 mL), and the aqueous layer was further extracted with dichloromethane (3 \times 50 mL). The combined organics were dried over anhydrous Na_2SO_4 , filtered, and concentrated under reduced pressure. The residue was purified by column chromatography on silica gel (EtOAc + 10% MeOH/hexanes) to afford the title compound contaminated with ethyl [3-(1-methyl-1H-pyrazol-4-yl)-5-oxo-5H-benzo[4,5]cyclohepta[1,2-b]pyridin-7-yl]acetate (109 mg, 0.203 mmol, 72% purity, 30% yield) as a yellow oil. MS (APCI) calcd for $\text{C}_{23}\text{H}_{22}\text{N}_3\text{O}_3$ $[\text{M} + \text{H}]^+$, 388.2; found, 388.1.

Ethyl Hydroxy[3-(1-methyl-1H-pyrazol-4-yl)-5-oxo-5H-benzo[4,5]cyclohepta[1,2-b]pyridin-7-yl]acetate (6b). Ethyl [3-(1-methyl-1H-pyrazol-4-yl)-5-oxo-5H-benzo[4,5]cyclohepta[1,2-b]pyridin-7-yl]acetate (250 mg, 0.670 mmol) was dissolved in THF (6.7 mL) and then cooled to -78 °C. LDA (0.670 mL, 1.34 mmol) was added dropwise, and the resulting solution was then stirred at -78 °C for 30 min. Then, racemic (10)-(camphorylsulfonyl)oxaziridine (384 mg, 1.67 mmol) was added dropwise as a solution in tetrahydrofuran (2.0 mL). After 15 min, the reaction mixture was neutralized with 1.5 mL of 1 M HCl and then partitioned between saturated aqueous sodium hydrogen carbonate (100 mL) and dichloromethane (50 mL), and the aqueous layer was further extracted with dichloromethane (3 \times 50 mL). The combined organics were dried over anhydrous Na_2SO_4 , filtered, and concentrated under reduced pressure. The residue was purified by preparative HPLC reverse phase (C-18), eluting with acetonitrile/water + 0.1% TFA, to afford the title compound (62.6 mg, 0.161 mmol, 24% yield) as a yellow solid. ^1H NMR (500 MHz, $\text{DMSO}-d_6$) δ 9.20 (d, $J = 2.0$ Hz, 1H), 8.54 (d, $J = 2.0$ Hz, 1H), 8.46 (s, 1H), 8.20 (d, $J = 1$ Hz, 1H), 8.13 (s, 1H), 7.80 (m, 2H), 7.38 (d, $J = 10.5$ Hz, 1H), 7.29 (d, $J = 10.5$ Hz, 1H), 6.33 (d, $J = 4.5$ Hz, 1H), 5.33 (d, $J = 4.5$ Hz, 1H), 4.09 (m, 2H), 3.88 (s, 3H), 1.12 (t, $J = 6.0$ Hz, 3H). MS (APCI) calcd for $\text{C}_{22}\text{H}_{20}\text{N}_3\text{O}_4$ $[\text{M} + \text{H}]^+$, 390.1; found, 390.1.

2-[3-(1-methyl-1H-pyrazol-4-yl)-5-oxo-5H-benzo[4,5]cyclohepta[1,2-b]pyridin-7-yl]propanamide (7a). Step 1: Ethyl 2-[3-(1-methyl-1H-pyrazol-4-yl)-5-oxo-5H-benzo[4,5]cyclohepta[1,2-b]pyridin-7-yl]propanoate contaminated with ethyl [3-(1-methyl-1H-pyrazol-4-yl)-5-oxo-5H-benzo[4,5]cyclohepta[1,2-b]pyridin-7-yl]acetate (109 mg, 0.281 mmol, 72% purity) was dissolved in THF (1125 μL). NaOH (1.0N, 563 μL , 0.563 mmol) was added, and the resulting suspension was stirred at room temperature for 30 min before heating to reflux. Then, the reaction was cooled to room temperature, neutralized with HCl (1.0N, 563 μL , 0.563 mmol), concentrated under reduced pressure, filtered, and dried under reduced pressure to afford 2-[3-(1-methyl-1H-pyrazol-4-yl)-5-oxo-5H-benzo[4,5]cyclohepta[1,2-b]pyridin-7-yl]propanoic acid contaminated with [3-(1-methyl-1H-pyrazol-4-yl)-5-oxo-5H-benzo[4,5]cyclohepta[1,2-b]pyridin-7-yl]acetic acid (101 mg, 72% purity) as a yellow powder. MS (APCI) calcd for $\text{C}_{21}\text{H}_{17}\text{N}_3\text{O}_3$ $[\text{M} + \text{H}]^+$, 360.1; found, 360.1.

Step 2: 2-[3-(1-methyl-1H-pyrazol-4-yl)-5-oxo-5H-benzo[4,5]cyclohepta[1,2-b]pyridin-7-yl]propanoic acid (101 mg, 0.281 mmol) was suspended in dichloromethane (2.81 mL) at room temperature. Then, triethylamine (0.196 mL, 1.41 mmol) was added followed by

HATU (214 mg, 0.562 mmol) and finally ammonia in isopropyl alcohol (2.0 M, 0.562 mL, 1.12 mmol). The mixture was allowed to stir at room temperature for 1 h and then concentrated under reduced pressure. The residue was purified by preparative HPLC reverse phase (C-18), eluting with acetonitrile/water + 0.1% TFA, to afford the title compound (40 mg, 0.11 mmol, 40% yield) as a yellow solid. ^1H NMR (500 MHz, $\text{DMSO}-d_6$) δ 9.19 (d, $J = 2.0$ Hz, 1H), 8.52 (d, $J = 1.5$ Hz, 1H), 8.45 (s, 1H), 8.13 (s, 1H), 8.08 (s, 1H), 7.74 (s, 2H), 7.51 (s, 1H), 7.37 (d, $J = 10.5$ Hz, 1H), 7.27 (d, $J = 10.0$ Hz, 1H), 6.92 (s, 1H), 3.88 (s, 3H), 3.75 (q, $J = 5.5$ Hz, 1H), 1.36 (d, $J = 6.0$ Hz). MS (APCI) calcd for $\text{C}_{21}\text{H}_{19}\text{N}_4\text{O}_2$ $[\text{M} + \text{H}]^+$, 359.1; found, 359.1.

2-Hydroxy-2-[3-(1-methyl-1H-pyrazol-4-yl)-5-oxo-5H-benzo[4,5]cyclohepta[1,2-b]pyridin-7-yl]acetamide (7b). Step 1: Ethyl hydroxy[3-(1-methyl-1H-pyrazol-4-yl)-5-oxo-5H-benzo[4,5]cyclohepta[1,2-b]pyridin-7-yl]acetate (63 mg, 0.16 mmol) was suspended in NaOH (1.0N, 322 μL , 0.322 mmol) and THF (643 μL) with stirring at room temperature. After 90 min, the mixture was neutralized with 1N HCl (322 mL) to form a yellow solution and then concentrated under reduced pressure to afford hydroxy[3-(1-methyl-1H-pyrazol-4-yl)-5-oxo-5H-benzo[4,5]cyclohepta[1,2-b]pyridin-7-yl]acetic acid as a yellow solid that was used directly in the next step. MS (APCI) calcd for $\text{C}_{20}\text{H}_{16}\text{N}_3\text{O}_4$ $[\text{M} + \text{H}]^+$, 362.1; found, 362.1.

Step 2: Triethylamine (55.9 μL , 0.401 mmol), HATU (31 mg, 0.080 mmol), and then ammonia in isopropyl alcohol (2.0 M, 80 μL , 0.161 mmol) were added to a stirring suspension of hydroxy[3-(1-methyl-1H-pyrazol-4-yl)-5-oxo-5H-benzo[4,5]cyclohepta[1,2-b]pyridin-7-yl]acetic acid (29 mg, 0.080 mmol) in dichloromethane (803 μL) at room temperature. The reaction was stirred overnight and then concentrated under reduced pressure. The residue was taken up in dichloromethane (803 μL) and to this was added triethylamine (55.9 μL , 0.401 mmol), HATU (31 mg, 0.080 mmol), and then ammonia in isopropyl alcohol (2.0 M, 80 μL , 0.16 mmol). After stirring for a further 24 h, the reaction was concentrated under reduced pressure. The residue was purified by preparative HPLC reverse phase (C-18), eluting with acetonitrile/water + 0.1% TFA, to afford the title compound (5 mg, 0.01 mmol, 17% yield) as a yellow solid. ^1H NMR (500 MHz, $\text{DMSO}-d_6$) δ 9.19 (d, $J = 2.0$ Hz, 1H), 8.53 (d, $J = 2.0$ Hz, 1H), 8.46 (s, 1H), 8.21 (d, $J = 1.0$ Hz, 1H), 8.13 (s, 1H), 7.84 (dd, $J = 6.5$, 1.5 Hz, 1H), 7.75 (d, $J = 7.0$ Hz), 7.51 (d, $J = 1.5$ Hz, 1H), 7.38 (d, $J = 10.5$ Hz, 1H), 7.29 (d, $J = 10.0$ Hz, 1H), 7.27 (d, $J = 1.0$ Hz, 1H), 6.30 (d, $J = 4.0$ Hz, 1H), 5.03 (d, $J = 4.0$ Hz, 1H). MS (APCI) calcd for $\text{C}_{20}\text{H}_{17}\text{N}_4\text{O}_3$ $[\text{M} + \text{H}]^+$, 361.1; found, 361.1.

Methyl [(Dimethylamino)sulfonyl]acetate (8a). Dimethylamine in THF (57.9 mL, 116 mmol) was dissolved in dichloromethane (29.0 mL) and cooled to 0 °C. Then, methyl (chlorosulfonyl)acetate (prepared according to ref 27) (10.0 g, 57.9 mmol) was added dropwise as a solution in dichloromethane (29.0 mL) while maintaining the temperature below 5 °C. The resulting solution was allowed to warm to room temperature over the course of 2 h. Then, brine (200 mL) was added and the aqueous phase was extracted with dichloromethane (3 \times 100 mL). The combined organics were dried over anhydrous Na_2SO_4 , filtered, and concentrated under reduced pressure. The residue was purified by column chromatography on silica gel (EtOAc/hexanes gradient) to afford the title compound (5.98 g, 33.0 mmol, 57% yield) as a yellow liquid. ^1H NMR (600 MHz, $\text{DMSO}-d_6$) δ 4.25 (s, 2H), 3.68 (s, 3H), 2.78 (s, 6H). MS (APCI) calcd for $\text{C}_5\text{H}_{12}\text{NO}_2\text{S}$ $[\text{M} + \text{H}]^+$, 182.0; found, 182.0.

Methyl [(Methyl(phenyl)amino)sulfonyl]acetate (8b). Chlorine gas was passed through a suspension of ice (230 g), CH_2Cl_2 (457 mL), and methyl thioglycolate (86.0 mL, 942 mmol), with external cooling with an ice/water bath to maintain an internal temperature below 30 °C. After approximately 6 h, the yellow/green color of the dissolved chlorine persisted for 30 min after gas flow was stopped and passing additional chlorine gas was no longer exothermic. The cooling bath was then removed, and the biphasic mixture was allowed to stir at ambient temperature for 1 h before being sparged with nitrogen for 20 min. The layers were then separated, and the organic phase was dried over Na_2SO_4 , filtered, and concentrated under reduced pressure to provide the intermediate methyl (chlorosulfonyl)acetate (160 g, 927 mmol) as a yellow oil. A portion of the intermediate methyl

(chlorosulfonyl)acetate (100 g, 579 mmol) was added dropwise as a solution in CH_2Cl_2 (290 mL) to a stirring -15°C solution of *N*-methylaniline (124 g, 1159 mmol) dissolved in CH_2Cl_2 (290 mL). The rate of addition was adjusted to maintain the internal temperature below 5°C . After the addition was complete, the reaction mixture was allowed to warm to room temperature over the course of 2 h, and 1 M HCl (1000 mL) was added and the aqueous phase was extracted with dichloromethane (2×500 mL). The combined organics were dried over anhydrous Na_2SO_4 , filtered, and concentrated under reduced pressure. The resulting oil was seed crystallized to afford a brown solid. Recrystallization from hot ethanol (320 mL) provided the title compound (110 g, 152 mmol, 78% yield) as an off-white solid. ^1H NMR (600 MHz, $\text{DMSO}-d_6$) δ 7.40 (m, 4H), 7.31 (m, 1H), 4.30 (s, 2H), 3.65 (s, 3H), 3.26 (s, 3H). MS (APCI) calcd for $\text{C}_{25}\text{H}_{21}\text{N}_4\text{O}_3\text{S}$ $[\text{M} + \text{H}]^+$, 444.1; found, 444.0.

1-(3-Chloro-5-oxo-5H-benzo[4,5]cyclohepta[1,2-b]pyridin-7-yl)-N,N-dimethylmethanesulfonamide (9a). Step 1: A 200 mL round-bottom flask was charged with methyl [(dimethylamino)sulfonyl]acetate (5.26 g, 29.0 mmol) and dioxane (77 mL), cooled to 0°C , and then sodium hydride (2.32 g, 58.0 mmol) was added in one portion. After 15 min, the mixture was warmed to room temperature and 7-bromo-3-chloro-5H-benzo[4,5]cyclohepta[1,2-b]pyridin-5-one (6.20 g, 19.34 mmol) was added followed by $\text{Pd}_2(\text{dba})_3$ (0.71 g, 0.77 mmol) and triphenylphosphine (1.22 g, 4.64 mmol). The resulting suspension was degassed by sparging with nitrogen for 30 min. Then, the mixture was heated to 70°C and left to stir overnight. The reaction was then cooled to room temperature, poured into brine (500 mL), and extracted with dichloromethane (3×150 mL). The combined organics were then dried over anhydrous Na_2SO_4 , filtered, and concentrated under reduced pressure. The residue was purified by column chromatography on silica gel (EtOAc/hexanes gradient) to afford methyl (3-chloro-5-oxo-5H-benzo[4,5]cyclohepta[1,2-b]pyridin-7-yl)[(dimethylamino)sulfonyl]acetate (2.04 g, 4.85 mmol, 25% yield) as a yellow oil that solidified to a yellow solid upon standing. ^1H NMR (600 MHz, $\text{DMSO}-d_6$) δ 9.00 (d, 1H), 8.49 (d, 1H), 8.47 (d, 1H), 8.07 (dd, 1H), 7.88 (d, 1H), 7.48 (d, 1H), 7.34 (d, 1H), 6.05 (s, 1H), 3.75 (s, 3H), 2.68 (s, 6H). MS (APCI) calcd for $\text{C}_{19}\text{H}_{18}\text{ClN}_2\text{O}_5\text{S}$ $[\text{M} + \text{H}]^+$, 421.1; found, 421.0.

Step 2: Methyl (3-chloro-5-oxo-5H-benzo[4,5]cyclohepta[1,2-b]pyridin-7-yl)[(dimethylamino)sulfonyl]acetate (2.04 g, 4.85 mmol) was dissolved in a mixture of AcOH (24.2 mL) and 6N HCl (24.24 mL) and heated to 100°C for 3 h. The solution was then cooled to room temperature, basified with saturated aqueous sodium hydrogen carbonate, and extracted with dichloromethane (3×50 mL). The combined organics were dried over anhydrous Na_2SO_4 , filtered, and concentrated under reduced pressure. The residue was purified by column chromatography on silica gel (EtOAc/hexanes gradient) to afford the title compound (1.44 g, 3.97 mmol, 82% yield) as a yellow solid. ^1H NMR (600 MHz, $\text{DMSO}-d_6$) δ 8.99 (d, 1H), 8.48 (d, 1H), 8.21 (s, 1H), 7.84 (m, 2H), 7.49 (d, 1H), 7.33 (d, 1H), 4.63 (s, 2H), 2.74 (s, 6H). MS (APCI) calcd for $\text{C}_{17}\text{H}_{16}\text{ClN}_2\text{O}_3\text{S}$ $[\text{M} + \text{H}]^+$, 363.1; found, 363.1.

Methyl (3-Chloro-5-oxo-5H-benzo[4,5]cyclohepta[1,2-b]pyridin-7-yl)[methyl(phenyl)sulfamoyl]acetate. Sodium *tert*-butoxide (8.99 g, 94 mmol) was added in one portion to a 250 mL flask containing methyl {[methyl(phenyl)amino]sulfonyl}acetate (7.59 g, 31.2 mmol) and dioxane (125 mL) at room temperature. After 15 min, 7-bromo-3-chloro-5H-benzo[4,5]cyclohepta[1,2-b]pyridin-5-one (10.00 g, 31.2 mmol) was added, followed by palladium(II) acetate (0.35 g, 1.6 mmol) and tri-*tert*-butylphosphonium tetrafluoroborate (1.36 g, 4.68 mmol). The resulting suspension was degassed by sparging with nitrogen for 30 min. Then the mixture was heated to 90°C in a prewarmed bath and left to stir for 1 h. Then the reaction mixture was cooled to room temperature, acidified with 1N HCl (100 mL), basified with saturated aqueous sodium hydrogen carbonate (400 mL), and extracted with dichloromethane (3×250 mL). The combined organics were dried over anhydrous Na_2SO_4 , filtered, and concentrated under reduced pressure. The residue was purified by column chromatography on silica gel (EtOAc/hexanes gradient) to afford the title compound (11.8 g, 24.4 mmol, 78% yield) as a yellow

foam. ^1H NMR (600 MHz, $\text{DMSO}-d_6$) δ 8.99 (d, 1H), 8.46 (d, 1H), 8.42 (d, 1H), 8.03 (dd, 1H), 7.81 (d, 1H), 7.44 (d, 1H), 7.33 (d, 1H), 7.22 (m, 2H), 7.17 (m, 2H), 7.11 (m, 1H), 6.10 (s, 1H), 3.71 (s, 3H), 3.20 (s, 3H). MS (APCI) calcd for $\text{C}_{24}\text{H}_{20}\text{ClN}_2\text{O}_5\text{S}$ $[\text{M} + \text{H}]^+$, 483.1; found, 483.0.

1-(3-Chloro-5-oxo-5H-benzo[4,5]cyclohepta[1,2-b]pyridin-7-yl)-N-methyl-N-phenylmethanesulfonamide (9b). Sodium *tert*-butoxide (47.4 g, 493 mmol) was added in one portion to a 1 L flask containing methyl {[methyl(phenyl)amino]sulfonyl}acetate (40.0 g, 164 mmol) and dissolved in dioxane (658 mL) at 0°C . After 15 min, 7-bromo-3-chloro-5H-benzo[4,5]cyclohepta[1,2-b]pyridin-5-one (52.7 g, 164 mmol) was added, followed by palladium(II) acetate (1.85 g, 8.22 mmol) and tri-*tert*-butylphosphonium tetrafluoroborate (7.16 g, 24.7 mmol). The resulting suspension was degassed by sparging with nitrogen for 30 min. Then the mixture was heated to 90°C in a prewarmed bath and left to stir for 1 h. Then the reaction flask was cooled to 50°C , 1N NaOH (500 mL) was added, and the solution was stirred for 1 h. Then the solution was diluted with saturated aqueous sodium hydrogen carbonate (800 mL) and extracted with dichloromethane (3×500 mL). The combined organics were dried over anhydrous Na_2SO_4 , filtered, and concentrated under reduced pressure. The residue was purified by column chromatography (EtOAc/hexanes gradient) to afford the title compound (51.65 g, 122.0 mmol, 74% yield) as a pale-yellow solid. ^1H NMR (600 MHz, $\text{DMSO}-d_6$) δ 8.99 (d, 1H), 8.47 (m, 1H), 8.17 (s, 1H), 7.81 (s, 2H), 7.47 (d, 1H), 7.32 (m, 5H), 7.21 (m, 1H), 4.75 (s, 2H), 3.24 (s, 3H). MS (APCI) calcd for $\text{C}_{22}\text{H}_{18}\text{ClN}_2\text{O}_3\text{S}$ $[\text{M} + \text{H}]^+$, 425.1; found, 425.0.

N,N-Dimethyl-1-[3-(1-methyl-1H-pyrazol-4-yl)-5-oxo-5H-benzo[4,5]cyclohepta[1,2-b]pyridin-7-yl]methanesulfonamide (10a). 1-(3-Chloro-5-oxo-5H-benzo[4,5]cyclohepta[1,2-b]pyridin-7-yl)-N,N-dimethylmethanesulfonamide (1.44 g, 3.97 mmol), 1-methyl-4-(4,4,5,5-tetramethyl-1,3,2-dioxaborolan-2-yl)-1H pyrazole (1.24 g, 5.95 mmol), tri-*tert*-butylphosphonium tetrafluoroborate (104 mg, 0.357 mmol), $\text{Pd}_2(\text{dba})_3$ (145 mg, 0.159 mmol), and potassium fluoride (761 mg, 13.1 mmol) were combined as solids and then placed under a nitrogen atmosphere. DMF (39.7 mL) was added, and the resulting suspension was heated to 130°C and left to stir for 1 h. Then the reaction was cooled to room temperature and partitioned between saturated aqueous sodium hydrogen carbonate (250 mL) and dichloromethane (250 mL). The organic layer was dried over anhydrous Na_2SO_4 , filtered, and concentrated under reduced pressure. The residue was purified by column chromatography on silica (EtOAc + 10% MeOH/hexanes gradient) to afford the title compound (1.33 g, 3.25 mmol, 82% yield) as a yellow solid. ^1H NMR (600 MHz, $\text{DMSO}-d_6$) δ 9.21 (d, 1H), 8.54 (d, 1H), 8.47 (s, 1H), 8.19 (s, 1H), 8.14 (s, 1H), 7.81 (m, 2H), 7.40 (d, 1H), 7.32 (d, 1H), 4.63 (s, 2H), 3.88 (s, 3H), 2.74 (s, 6H). MS (APCI) calcd for $\text{C}_{21}\text{H}_{21}\text{N}_4\text{O}_3\text{S}$ $[\text{M} + \text{H}]^+$, 409.1; found, 409.1.

N-Methyl-1-[3-(1-methyl-1H-pyrazol-4-yl)-5-oxo-5H-benzo[4,5]cyclohepta[1,2-b]pyridin-7-yl]-N-phenylmethanesulfonamide (10b). 1-(3-Chloro-5-oxo-5H-benzo[4,5]cyclohepta[1,2-b]pyridin-7-yl)-N-methyl-N-phenylmethanesulfonamide (4.40 g, 10.4 mmol), 1-methyl-4-(4,4,5,5-tetramethyl-1,3,2-dioxaborolan-2-yl)-1H pyrazole (2.59 g, 12.4 mmol), potassium fluoride (1.99 g, 34.2 mmol), tri-*tert*-butylphosphonium tetrafluoroborate (0.27 g, 0.93 mmol), and $\text{Pd}_2(\text{dba})_3$ (379 mg, 0.414 mmol) were combined as solids and placed under a nitrogen atmosphere. DMF (104 mL) was added, the mixture was degassed, and then the reaction was heated to 130°C with stirring for 2 h. After cooling to room temperature, the mixture was poured into aqueous sodium hydrogen carbonate (saturated, 250 mL) and extracted with dichloromethane (4×250 mL). The organic extracts were combined, dried over Na_2SO_4 , and concentrated under reduced pressure. The residue was then dissolved in hot dioxane (500 mL). Hexanes were added until a precipitate formed. After standing at room temperature overnight, the precipitate was collected to afford the title compound (2.30 g, 4.90 mmol, 47% yield) as a gray solid. ^1H NMR (600 MHz, $\text{DMSO}-d_6$) δ 9.22 (d, 1H), 8.53 (d, 1H), 8.47 (s, 1H), 8.15 (s, 1H), 8.14 (d, 1H), 7.78 (m, 2H), 7.39 (d, 1H), 7.32 (m, 5H), 7.20 (m, 1H), 4.75 (s, 2H), 3.88 (s, 3H),

3.23 (s, 3H). MS (APCI) calcd for $C_{21}H_{21}N_4O_3S$ $[M + H]^+$, 409.1; found, 409.1.

1-[3-(1-Methyl-1H-pyrazol-4-yl)-5-oxo-5H-benzo[4,5]-cyclohepta[1,2-b]pyridin-7-yl]-N-phenylmethanesulfonamide (11h). Cesium carbonate (80 mg, 0.25 mmol) was added to a solution of *N,N*-dimethyl-1-[3-(1-methyl-1H-pyrazol-4-yl)-5-oxo-5H-benzo[4,5]-cyclohepta[1,2-b]pyridin-7-yl]methanesulfonamide (50 mg, 0.12 mmol) and aniline (559 μ L, 6.12 mmol) in dioxane (1113 μ L) and water (111 μ L) in a sealed pressure vessel. The vial was then sealed, and the mixture was heated to 180 °C for 3 h. After cooling to room temperature, the reaction mixture was concentrated under reduced pressure. The residue was purified by preparative HPLC reverse phase (C-18), eluting with acetonitrile/water + 0.1% TFA, to afford the title compound (7.3 mg, 0.016 mmol, 13% yield) as a yellow solid. 1H NMR (600 MHz, DMSO- d_6) δ 9.84 (br s, 1H), 9.22 (d, 1H), 8.51 (d, 1H), 8.48 (s, 1H), 8.15 (s, 1H), 8.04 (d, 1H), 7.76 (d, 1H), 7.63 (dd, 1H), 7.38 (d, 1H), 7.32 (d, 1H), 7.27 (m, 2H), 7.16 (dd, 2H), 7.00 (m, 1H), 4.68 (s, 2H), 3.89 (s, 3H). MS (APCI) calcd for $C_{25}H_{21}N_4O_3S$ $[M + H]^+$, 457.1; found, 457.1. **11a–e**, **11i–k**, and **11p–q** were prepared by the same method as **11h** in library format.

***N*-[trans-2-Aminocyclohexyl]-1-[3-(1-methyl-1H-pyrazol-4-yl)-5-oxo-5H-benzo[4,5]cyclohepta[1,2-b]pyridin-7-yl]methanesulfonamide (11g).** *N*-methyl-1-[3-(1-methyl-1H-pyrazol-4-yl)-5-oxo-5H-benzo[4,5]cyclohepta[1,2-b]pyridin-7-yl]-*N*-phenylmethanesulfonamide (100 mg, 0.213 mmol) and (1*R*,2*R*)-(-)-1,2-diaminocyclohexane (109 mg, 0.956 mmol) were dissolved in *N*-methyl-2-pyrrolidinone (2.0 mL) in a 5 mL sealed pressure vessel. The vial was capped and heated to 190 °C for 0.5 h. The mixture was diluted with MeOH and purified by preparative HPLC reverse phase (C-18), eluting with acetonitrile/water + 0.05% TFA to afford the title compound (80 mg, 0.17 mmol, 79% yield) as a yellow solid. 1H NMR (500 MHz, CDCl₃) δ 9.02 (s, 1H), 8.55 (s, 1H), 8.33 (s, 1H), 7.92 (s, 1H), 7.82 (s, 2H), 7.61 (d, $J = 7.9$, 1H), 7.37 (d, $J = 12.4$, 1H), 7.22 (d, $J = 12.5$, 1H), 4.55 (d, $J = 13.5$, 1H), 4.43 (d, $J = 13.7$, 1H), 3.99 (s, 3H), 2.97 (s, 1H), 2.37 (t, $J = 10.3$, 1H), 2.23 (s, 1H), 2.01 (s, 2H), 1.96 (d, $J = 12.7$, 1H), 1.72 (s, 2H), 1.23 (m, 5H). MS (APCI) calcd for $C_{25}H_{27}N_5O_3S$ $[M + H]^+$, 478.2; found, 477.8. **11f**, **11l**, **11m**, **11o**, **11s**, **11u**, and **11v** were prepared in library format in analogy to **11g**.

1-[3-(1-Methyl-1H-pyrazol-4-yl)-5-oxo-5H-benzo[4,5]-cyclohepta[1,2-b]pyridin-7-yl]-*N*-[(2-methylpyrimidin-4-yl)methyl]methanesulfonamide (11n). Step 1: *N*-Methyl-1-[3-(1-methyl-1H-pyrazol-4-yl)-5-oxo-5H-benzo[4,5]cyclohepta[1,2-b]pyridin-7-yl]-*N*-phenylmethanesulfonamide (1.30 g, 2.76 mmol), methanesulfonic acid (3.7 mL), and water (7.4 mL) were placed in a sealed pressure vessel. The mixture was heated at 110 °C for 43 h. The reaction mixture was cooled to ambient temperature, and solids were collected by filtration, washed with water (20 mL) and EtOAc (20 mL), and dried to afford 1-[3-(1-methyl-1H-pyrazol-4-yl)-5-oxo-5H-benzo[4,5]cyclohepta[1,2-b]pyridin-7-yl]-*N*-phenylmethanesulfonic acid (850 mg, 2.23 mmol, 81% yield) as off-white solid that was used without further purification. 1H NMR (600 MHz, DMSO- d_6) δ 9.20 (d, 1H), 8.68 (d, 1H), 8.49 (s, 1H), 8.16 (s, 1H), 8.07 (s, 1H), 7.73 (dd, 1H), 7.68 (d, 1H), 7.43 (d, 1H), 7.22 (d, 1H), 3.90 (s, 2H), 3.87 (s, 3H). MS (APCI) calcd for $C_{19}H_{16}N_3O_4S$ $[M + H]^+$, 382.1; found, 382.1.

Step 2: In a 10 mL round-bottom flask charged with 1-[3-(1-methyl-1H-pyrazol-4-yl)-5-oxo-5H-benzo[4,5]cyclohepta[1,2-b]pyridin-7-yl]-*N*-phenylmethanesulfonic acid (50 mg, 0.13 mmol) in dichloromethane (1.3 mL) was added DMF (12 μ L, 0.16 mmol), followed by oxalyl chloride ((2 M in dichloromethane, 328 μ L, 0.65 mmol). The resulting mixture was stirred for 1.5 h, and then volatiles were removed in vacuo. The crude residue was taken up in dichloromethane (1.3 mL), and 1-(2-methylpyrimidin-4-yl)-methanamine dihydrochloride (103 mg, 0.524 mmol) was added. The mixture was stirred for 5 min, followed by addition of triethylamine (146 μ L, 1.05 mmol), and stirred for 30 min. The crude reaction mixture was directly subjected to silica gel column chromatography (25 g, 0–100% 10:1:0.5 EtOAc/MeOH/Et₃N in hexanes) to afford 1-[3-(1-methyl-1H-pyrazol-4-yl)-5-oxo-5H-benzo[4,5]cyclohepta[1,2-b]pyridin-7-yl]-*N*-[(2-methylpyrimidin-4-yl)-

methyl]methanesulfonamide (20 mg, 0.041 mmol, 31% yield). 1H NMR (600 MHz, CDCl₃) δ 8.95 (d, 1H), 8.50 (d, 1H), 8.42 (d, 1H), 8.18 (d, 1H), 7.88 (s, 1H), 7.79 (s, 1H), 7.73 (dd, 1H), 7.52 (d, 1H), 7.25 (d, 1H), 7.11 (d, 1H), 7.03 (d, 1H), 4.45 (s, 2H), 4.25 (s, 2H), 3.97 (s, 3H), 2.63 (s, 3H). MS (APCI) calcd for $C_{25}H_{23}N_6O_3S$ $[M + H]^+$, 487.1; found, 487.1.

1-[3-(1-Methyl-1H-pyrazol-4-yl)-5-oxo-5H-benzo[4,5]-cyclohepta[1,2-b]pyridin-7-yl]-*N*-(pyridin-2-ylmethyl)methanesulfonamide (11r). Step 1: 2-Aminomethylpyridine (55.9 mL, 546 mmol) was added to a solution of 1-(3-chloro-5-oxo-5H-benzo[4,5]cyclohepta[1,2-b]pyridin-7-yl)-*N*-methyl-*N*-phenylmethanesulfonamide (51.6 g, 121 mmol) in *N*-methyl-2-pyrrolidinone (1214 mL) at room temperature. The solution was then heated to 130–135 °C for 2 h in a prewarmed oil bath. The solution was then cooled to room temperature and poured into aqueous sodium hydrogen carbonate (saturated, 3.0 L) and ice-water (500 mL) and extracted with ethyl acetate (3 \times 500 mL). The combined organics were dried over anhydrous Na₂SO₄, filtered, and concentrated under reduced pressure. The residue was purified by column chromatography on silica gel (EtOAc/hexanes gradient) to afford 1-(3-chloro-5-oxo-5H-benzo[4,5]cyclohepta[1,2-b]pyridin-7-yl)-*N*-(pyridin-2-ylmethyl)methanesulfonamide (37.2 g, 87.0 mmol, 72% yield) as a yellow solid. 1H NMR (600 MHz, DMSO- d_6) δ 8.99 (d, 1H), 8.47 (d, 1H), 8.46 (m, 1H), 8.16 (d, 1H), 7.81 (m, 3H), 7.76 (m, 1H), 7.49 (d, 1H), 7.38 (d, 1H), 7.32 (d, 1H), 7.25 (m, 1H), 4.63 (s, 2H), 4.22 (d, 2H). MS (APCI) calcd for $C_{21}H_{17}ClN_5O_3S$ $[M + H]^+$, 426.1; found, 426.0.

Step 2: 1-(3-Chloro-5-oxo-5H-benzo[4,5]cyclohepta[1,2-b]pyridin-7-yl)-*N*-(pyridin-2-ylmethyl)methanesulfonamide (22.04 g, 51.80 mmol), lithium 2-hydroxy-4,4,5,5-tetramethyl-2-(1-methyl-1H-pyrazol-4-yl)-1,3,2-dioxaborolan-2-uide hydrate (25.3 g, 88.0 mmol), Pd₂(dba)₃ (2.37 g, 2.59 mmol), and tricyclohexylphosphine (1.81 g, 6.47 mmol) were placed in a flask under an atmosphere of argon. DMF (518 mL) was added, and argon was bubbled through the solution for several minutes. The solution was then heated at 100 °C for 4 h. The mixture was cooled to room temperature, poured into aqueous sodium hydrogen carbonate (saturated, 70 mL), and extracted with ethyl acetate (2 \times 75 mL). The combined organics were dried over anhydrous Na₂SO₄, filtered, and concentrated under reduced pressure. The residue was purified by column chromatography on silica gel, eluting with EtOAc + 10% MeOH + 1% Et₃N/hexanes gradient to afford the title compound (17.3 g, 36.7 mmol, 71% yield) as a pale-yellow solid. 1H NMR (600 MHz, DMSO- d_6) δ 9.21 (d, 1H), 8.53 (d, 1H), 8.47 (m, 1H), 8.46 (m, 1H), 8.15 (d, 1H), 8.14 (s, 1H), 7.78 (m, 4H), 7.39 (m, 2H), 7.32 (d, 1H), 7.24 (m, 1H), 4.63 (s, 2H), 4.22 (d, 1H), 3.88 (s, 3H). MS (APCI) calcd for $C_{25}H_{21}N_5O_3S$ $[M + H]^+$, 472.1; found, 472.1.

1-[3-(1-Methyl-1H-pyrazol-4-yl)-5-oxo-5H-benzo[4,5]-cyclohepta[1,2-b]pyridin-7-yl]-*N*-[(1-oxidopyridin-2-yl)methyl]methanesulfonamide (11t). 3-Chloroperoxybenzoic acid (26 mg, 0.11 mmol) was added to a solution of 1-[3-(1-methyl-1H-pyrazol-4-yl)-5-oxo-5H-benzo[4,5]cyclohepta[1,2-b]pyridin-7-yl]-*N*-(pyridin-2-ylmethyl)methanesulfonamide (50 mg, 0.11 mmol) in dichloromethane (1.06 mL) at 0 °C. After 15 min, the reaction was allowed to warm to room temperature and stirring was continued for 6 h. Then, aqueous sodium hydrogen carbonate (saturated, 50 mL) was added, and the mixture was extracted with dichloromethane (3 \times 50 mL). The combined organic extracts were washed with aqueous sodium hydrogen carbonate (saturated, 2 \times 75 mL), dried over anhydrous sodium sulfate, and concentrated under reduced pressure. The residue was purified by preparative HPLC reverse phase (C-18), eluting with acetonitrile/water + 0.05% TFA, to afford the title compound as a yellow solid. 1H NMR (600 MHz, DMSO- d_6) δ 9.21 (d, 1H), 8.53 (d, 1H), 8.47 (s, 1H), 8.25 (d, 1H), 8.17 (s, 1H), 8.14 (s, 1H), 7.80 (m, 3H), 7.46 (d, 1H), 7.40 (d, 1H), 7.34 (m, 3H), 4.71 (s, 2H), 4.27 (d, 2H), 3.88 (s, 3H). MS (APCI) calcd for $C_{25}H_{21}N_5O_4S$ $[M + H]^+$, 488.1; found, 488.1.

3-Chloro-7-[[2-(trimethylsilyl)ethoxy]methyl]-5H-benzo[4,5]cyclohepta[1,2-b]pyridin-5-one. 7-Bromo-3-chloro-5H-benzo[4,5]cyclohepta[1,2-b]pyridin-5-one (5.00 g, 15.6 mmol), potassium 2-(trimethylsilyl)ethoxymethyltrifluoroborate (4.46 g,

18.7 mmol), palladium(II) acetate (175 mg, 0.780 mmol), RuPhos (728 mg, 1.56 mmol), and Cs_2CO_3 (15.25 g, 46.80 mmol) were taken up in 1,4-dioxane (55 mL)/water (5.5 mL). The flask was evacuated and backfilled with N_2 three times before stirring at 100 °C for 18 h. Additional palladium(II) acetate (88 mg, 0.39 mmol) and RuPhos (364 mg, 0.780 mmol) were added, the flask was evacuated and backfilled with N_2 three times before stirring at 100 °C for an additional 24 h. The reaction mixture was cooled to room temperature, saturated NH_4Cl was added, and the products extracted into dichloromethane. The combined organic extracts were washed with brine, dried over MgSO_4 , filtered, and concentrated in vacuo. Purification of the residue by flash chromatography (2–20% EtOAc/hexanes) gave 3-chloro-7-[[2-(trimethylsilyl)ethoxy]methyl]-5H-benzo[4,5]cyclohepta[1,2-b]pyridin-5-one (3.22 g, 8.66 mmol, 56% yield) as a yellow solid. ^1H NMR (600 MHz, $\text{DMSO}-d_6$) δ 8.95 (d, J = 2.4 Hz, 1 H), 8.42 (d, J = 2.4 Hz, 1 H), 8.07 (s, 1 H), 7.77 (d, J = 7.8 Hz, 1 H), 7.72 (dd, J = 7.8 and 1.8 Hz, 1 H), 7.44 (d, J = 12.0 Hz, 1 H), 7.25 (d, J = 12.0 Hz, 1 H), 4.56 (s, 2 H), 3.56 (t, J = 7.8 Hz, 2 H), 0.92 (t, J = 7.8 Hz, 2 H), -0.03, (s, 9 H). MS (APCI) calcd for $\text{C}_{20}\text{H}_{23}\text{ClNO}_2\text{Si}$ [$\text{M} + \text{H}$] $^+$, 372.1; found, 372.1.

3-Chloro-7-(hydroxymethyl)-5H-benzo[4,5]cyclohepta[1,2-b]pyridin-5-one. 3-Chloro-7-[[2-(trimethylsilyl)ethoxy]methyl]-5H-benzo[4,5]cyclohepta[1,2-b]pyridin-5-one (2.32 g, 6.24 mmol) was taken up in dichloromethane (12 mL) and cooled to 0 °C. Boron trifluoride etherate (3.95 mL, 31.2 mmol) was added before slowly warming to room temperature and stirring for 18 h. Saturated NaHCO_3 was added, and the resulting precipitate collected by filtration, washing with water and dichloromethane. The crude solid was recrystallized from dichloromethane to give 3-chloro-7-(hydroxymethyl)-5H-benzo[4,5]cyclohepta[1,2-b]pyridin-5-one (367 mg, 1.35 mmol, 22% yield) as a yellow solid (1st crop). The mother liquor was concentrated in vacuo while loading onto silica and purification by flash chromatography (12–100% EtOAc/hexanes) gave 3-chloro-7-(hydroxymethyl)-5H-benzo[4,5]cyclohepta[1,2-b]pyridin-5-one (415 mg, 1.53 mmol, 25% yield) as a yellow solid (2nd crop). The dichloromethane filtrate was concentrated in vacuo while loading onto MgSO_4 and purification by flash chromatography (12–100% EtOAc/hexanes) gave 3-chloro-7-(hydroxymethyl)-5H-benzo[4,5]cyclohepta[1,2-b]pyridin-5-one (0.37 g, 1.4 mmol, 22% yield) as a yellow solid (3rd crop). ^1H NMR (600 MHz, $\text{DMSO}-d_6$) δ 8.96 (d, J = 2.4 Hz, 1 H), 8.45 (d, J = 2.4 Hz, 1 H), 8.11 (s, 1 H), 7.77–7.73 (m, 2 H), 7.45 (d, J = 12.6 Hz, 1 H), 7.26 (d, J = 12.6 Hz, 1 H), 5.46 (t, J = 5.4 Hz, 1 H), 4.63 (d, J = 5.4 Hz, 2 H). MS (APCI) calcd for $\text{C}_{15}\text{H}_{11}\text{ClNO}_2$ [$\text{M} + \text{H}$] $^+$, 272.0; found, 272.0.

(3-Chloro-5-oxo-5H-benzo[4,5]cyclohepta[1,2-b]pyridin-7-yl)methylmethanesulfonate. 3-Chloro-7-(hydroxymethyl)-5H-benzo[4,5]cyclohepta[1,2-b]pyridin-5-one (0.32 g, 1.2 mmol) and Et_3N (0.230 mL, 1.65 mmol) were taken up in 1,4-dioxane (6 mL) and cooled to 0 °C. Methanesulfonyl chloride (0.11 mL, 1.4 mmol) was added before warming to room temperature and stirring for 2 h. Water was added and the products extracted into EtOAc. The combined organic extracts were washed with brine, dried over MgSO_4 , filtered, and concentrated in vacuo. The residue was recrystallized from EtOAc/hexanes to give (3-chloro-5-oxo-5H-benzo[4,5]cyclohepta[1,2-b]pyridin-7-yl)methylmethanesulfonate (0.32 g, 0.92 mmol, 78% yield) as yellow needles. ^1H NMR (600 MHz, $\text{DMSO}-d_6$) δ 8.97 (d, J = 2.4 Hz, 1 H), 8.44 (d, J = 2.4 Hz, 1 H), 8.18 (s, 1 H), 7.86 (s, 2 H), 7.48 (d, J = 12.6 Hz, 1 H), 7.31 (d, J = 12.6 Hz, 1 H), 5.42 (s, 2 H), 3.26 (s, 3 H). MS (APCI) calcd for $\text{C}_{16}\text{H}_{13}\text{ClNO}_4\text{S}$ [$\text{M} + \text{H}$] $^+$, 350.0; found, 349.9.

3-Chloro-7-[[2-(2-pyridin-2-ylethyl)thio]methyl]-5H-benzo[4,5]cyclohepta[1,2-b]pyridin-5-one. Sodium hydride (60 wt %, 9 mg, 0.2 mmol) was suspended in DMF (0.5 mL), and a solution of 2-pyridin-2-ylethanethiol (31 mg, 0.22 mmol) in DMF (0.2 mL) was added, forming a yellow solution. To this mixture was added a warm solution of (3-chloro-5-oxo-5H-benzo[4,5]cyclohepta[1,2-b]pyridin-7-yl)methylmethanesulfonate (60 mg, 0.17 mmol) in DMF (1 mL). The resulting mixture was stirred at room temperature for 30 min. Water was added and the products extracted into EtOAc. The combined organic extracts were washed with brine, dried over MgSO_4 , filtered,

and concentrated in vacuo. Purification of the residue by flash chromatography (12–100% EtOAc/hexanes) gave 3-chloro-7-[[2-(2-pyridin-2-ylethyl)thio]methyl]-5H-benzo[4,5]cyclohepta[1,2-b]pyridin-5-one (24 mg, 0.061 mmol, 36% yield) as a yellow gum. ^1H NMR (600 MHz, CDCl_3) δ 8.79 (d, J = 2.4 Hz, 1 H), 8.50–8.49 (m, 2 H), 8.15 (m, 1 H), 7.68 (dd, J = 7.8 and 1.8 Hz, 1 H), 7.58–7.54 (m, 2 H), 7.30 (d, J = 12.6 Hz, 1 H), 7.24 (d, J = 12.6 Hz, 1 H), 7.13–7.09 (m, 2 H), 3.80 (s, 2 H), 3.02 (t, J = 7.5 Hz, 2 H), 2.83 (t, J = 7.5 Hz, 2 H). MS (APCI) calcd for $\text{C}_{22}\text{H}_{18}\text{ClN}_2\text{OS}$ [$\text{M} + \text{H}$] $^+$, 393.1; found, 393.0.

3-Chloro-7-[[2-(2-pyridin-2-ylethyl)sulfonyl]methyl]-5H-benzo[4,5]cyclohepta[1,2-b]pyridin-5-one. 3-Chloro-7-[[2-(2-pyridin-2-ylethyl)thio]methyl]-5H-benzo[4,5]cyclohepta[1,2-b]pyridin-5-one (23 mg, 0.059 mmol) and MCPBA (77 wt %, 26 mg, 0.12 mmol) were stirred in dichloromethane (2 mL) at room temperature for 18 h. The reaction mixture was purified directly by flash chromatography (12–100% EtOAc/hexanes) to afford 3-chloro-7-[[2-(2-pyridin-2-ylethyl)sulfonyl]methyl]-5H-benzo[4,5]cyclohepta[1,2-b]pyridin-5-one (11 mg, 0.026 mmol, 44% yield) as an off-white solid. ^1H NMR (600 MHz, $\text{DMSO}-d_6$) δ 8.98 (d, J = 2.4 Hz, 1 H), 8.46–8.44 (m, 2 H), 8.02 (s, 1 H), 7.86–7.82 (m, 2 H), 7.71–7.68 (m, 1 H), 7.47 (d, J = 12.0 Hz, 1 H), 7.33–7.30 (m, 2 H), 7.23–7.20 (m, 1 H), 4.77 (s, 2 H), 3.52–3.48 (m, 2 H), 3.18–3.14 (m, 2 H). MS (APCI) calcd for $\text{C}_{22}\text{H}_{18}\text{ClN}_2\text{O}_3\text{S}$ [$\text{M} + \text{H}$] $^+$, 425.1; found, 425.0.

3-(1-Methyl-1H-pyrazol-4-yl)-7-[[2-(2-pyridin-2-ylethyl)sulfonyl]methyl]-5H-benzo[4,5]cyclohepta[1,2-b]pyridin-5-one (13). 1-Methyl-4-(4,4,5,5-tetramethyl-1,3,2-dioxaborolan-2-yl)-1H-pyrazole, lithium ate salt (10 mg, 0.042 mmol), $\text{Pd}(\text{dba})_3$ (1 mg, 1 μmol), and X-Phos (1 mg, 2 μmol) were added to a 2 mL sealed pressure vessel. The vial was evacuated and backfilled with N_2 three times before adding a solution of 3-chloro-7-[[2-(2-pyridin-2-ylethyl)sulfonyl]methyl]-5H-benzo[4,5]cyclohepta[1,2-b]pyridin-5-one (9 mg, 0.02 mmol) in DMF (1 mL). The resulting dark solution was heated to 150 °C for 20 min under microwave irradiation. Saturated NH_4Cl was added and the products extracted into EtOAc (twice). The combined organic extracts were washed with brine, dried over MgSO_4 , filtered, and concentrated in vacuo. Purification of the residue by flash chromatography (0–10% MeOH/EtOAc) afforded 3-(1-methyl-1H-pyrazol-4-yl)-7-[[2-(2-pyridin-2-ylethyl)sulfonyl]methyl]-5H-benzo[4,5]cyclohepta[1,2-b]pyridin-5-one (6 mg, 0.01 mmol, 60% yield) as a yellow solid. ^1H NMR (600 MHz, $\text{DMSO}-d_6$) δ 9.20 (d, J = 1.8 Hz, 1 H), 8.52 (d, J = 1.8 Hz, 1 H), 8.47–8.44 (m, 2 H), 8.18 (s, 1 H), 8.13 (s, 1 H), 7.83–7.79 (m, 2 H), 7.70–7.67 (m, 1 H), 7.39 (d, J = 12.6 Hz, 1 H), 7.34–7.31 (m, 2 H), 7.22–7.19 (m, 1 H), 4.77 (s, 2 H), 3.87 (s, 3 H), 3.52–3.48 (m, 2 H), 3.18–3.14 (m, 2 H). MS (APCI) calcd for $\text{C}_{26}\text{H}_{23}\text{N}_4\text{O}_3\text{S}$ [$\text{M} + \text{H}$] $^+$, 471.1; found, 471.1.

tert-Butyl 4-[(methylsulfonyl)oxy]piperidine-1-carboxylate. To a solution of *tert*-butyl 4-hydroxypiperidine-1-carboxylate (2.0 g, 9.9 mmol) and triethylamine (2.70 mL, 19.9 mmol) in dichloromethane (20 mL) at 0 °C was added methanesulfonyl chloride (1.15 mL, 14.9 mmol). The reaction mixture was allowed to warm to RT and stirred overnight. The reaction mixture was filtered, and the filtrate was diluted with dichloromethane and washed with 1N HCl and brine. The organic layer was dried over Na_2SO_4 , filtered, and dryloaded onto silica gel, and the crude residue was purified by flash chromatography (5–40% EtOAc/hexane) to provide *tert*-butyl 4-[(methylsulfonyl)oxy]piperidine-1-carboxylate (2.3 g, 8.2 mmol, 84% yield). ^1H NMR (500 MHz, CDCl_3) δ 4.87 (m, 1H), 3.69 (m, 2H), 3.30 (m, 2H), 3.03 (s, 3H), 1.95 (m, 2H), 1.80 (m, 2H), 1.45 (s, 9H).

tert-Butyl 4-(4-iodo-1H-pyrazol-1-yl)piperidine-1-carboxylate. To a solution of *tert*-butyl 4-[(methylsulfonyl)oxy]piperidine-1-carboxylate (1.0 g, 3.6 mmol) and 4-iodopyrazole (0.70 g, 3.6 mmol) in DMF (10 mL) was added NaH (60% mineral oil, 215 mg, 5.40 mmol). The reaction mixture was stirred under nitrogen until release of hydrogen gas ceased. The reaction was then placed in a microwave reactor and heated to 110 °C for 30 min. The reaction mixture was diluted with EtOAc and washed with brine. The organic layer was dried over Na_2SO_4 , filtered, and dryloaded onto silica gel, and the crude residue was purified by flash chromatography (5–40% EtOAc/hexane) to give *tert*-butyl 4-(4-iodo-1H-pyrazol-1-yl)piperidine-1-

carboxylate (740 mg, 1.96 mmol, 55% yield). ^1H NMR (500 MHz, DMSO- d_6) δ 7.98 (s, 1H), 7.51 (s, 1H), 4.34 (m, 1H), 4.01 (m, 2H), 2.86 (m, 2H), 1.94 (m, 2H), 1.72 (qd, 2H), 1.39 (s, 9H).

tert-Butyl 4-[4-(4,4,5,5-Tetramethyl-1,3,2-dioxaborolan-2-yl)-1H-pyrazol-1-yl]piperidine-1-carboxylate. *tert*-Butyl 4-(4-iodo-1H-pyrazol-1-yl)piperidine-1-carboxylate (1.6 g, 4.3 mmol), bis(pinacolato)diboron (1.5 g, 6.1 mmol), potassium acetate (1.70 g, 17.4 mmol), and 1,1'-bis(diphenylphosphino)ferrocene-palladium(II)-dichloride dichloromethane complex (0.2 g, 0.2 mmol) were combined in a vial and dissolved in DMSO (17 mL). The mixture was sparged with argon for 10 min and then heated to 80 °C for 3 h. The reaction mixture was diluted with EtOAc and filtered over Celite, and the filtrate was washed with brine. The organic layer was dried over Na_2SO_4 and filtered, and the crude residue was purified by flash chromatography (7–60% EtOAc/hexane) to give *tert*-butyl 4-[4-(4,4,5,5-tetramethyl-1,3,2-dioxaborolan-2-yl)-1H-pyrazol-1-yl]piperidine-1-carboxylate (1.2 g, 3.2 mmol, 73% yield). ^1H NMR (500 MHz, CDCl_3) δ 7.79 (s, 1H), 7.73 (s, 1H), 4.60 (m, 1H), 4.25 (m, 2H), 2.88 (m, 2H), 2.12 (m, 2H), 1.90 (m, 2H), 1.46 (s, 9H), 1.31 (s, 6H), 1.24 (s, 6H). MS (ESI) calcd for $\text{C}_{19}\text{H}_{32}\text{BN}_3\text{O}_4$ $[\text{M} + \text{H}]^+$, 378.3; found, 378.2.

tert-Butyl 4-[4-(5-Oxo-7-[(pyridin-2-ylmethyl)sulfamoyl]methyl)-5H-benzo[4,5]cyclohepta[1,2-*b*]pyridin-3-yl)-1H-pyrazol-1-yl]piperidine-1-carboxylate. 1-(3-Chloro-5-oxo-5H-benzo[4,5]cyclohepta[1,2-*b*]pyridin-7-yl)-*N*-(pyridin-2-ylmethyl)methanesulfonamide (84 mg, 0.20 mmol), *tert*-butyl 4-[4-(4,4,5,5-tetramethyl-1,3,2-dioxaborolan-2-yl)-1H-pyrazol-1-yl]piperidine-1-carboxylate (112 mg, 0.297 mmol), potassium fluoride (38 mg, 0.65 mmol), $\text{Pd}_2(\text{dba})_3$ (9 mg, 0.01 mmol), and tri-*t*-butylphosphonium tetrafluoroborate (6 mg, 0.02 mmol) were combined in a vial and dissolved in DMF (1.0 mL). The mixture was sparged with argon for 10 min and then heated to 130 °C overnight. The reaction mixture was diluted with EtOAc and washed with NH_4Cl and brine. The organic layer was dried over Na_2SO_4 , filtered, and dryloaded onto silica gel, and the crude residue was purified by flash chromatography (12–100% EtOAc/hexane, followed by 0–10% dichloromethane-MeOH) to give *tert*-butyl 4-[4-(5-oxo-7-[(pyridin-2-ylmethyl)sulfamoyl]methyl)-5H-benzo[4,5]cyclohepta[1,2-*b*]pyridin-3-yl)-1H-pyrazol-1-yl]piperidine-1-carboxylate (26 mg, 0.040 mmol, 20% yield) as an orange solid. ^1H NMR (500 MHz, DMSO- d_6) δ 9.24 (d, 1H), 8.65 (s, 1H), 8.58 (d, 1H), 8.48 (m, 1H), 8.19 (s, 1H), 8.15 (d, 1H), 7.80 (m, 4H), 7.40 (m, 2H), 7.34 (d, 1H), 7.25 (m, 1H), 4.64 (s, 2H), 4.44 (m, 1H), 4.23 (d, 1H), 4.02 (m, 2H), 3.15 (m, 2H), 2.05 (m, 2H), 1.82 (m, 2H), 1.40 (s, 9H). MS (ESI) calcd for $\text{C}_{33}\text{H}_{35}\text{N}_7\text{O}_5\text{S}$ $[\text{M} + \text{H}]^+$, 641.2; found, 641.3.

1-[5-Oxo-3-[1-(piperidin-4-yl)-1H-pyrazol-4-yl]-5H-benzo[4,5]cyclohepta[1,2-*b*]pyridin-7-yl]-*N*-(pyridin-2-ylmethyl)methanesulfonamide (16). To a solution of *tert*-butyl 4-[4-(5-oxo-7-[(pyridin-2-ylmethyl)sulfamoyl]methyl)-5H-benzo[4,5]cyclohepta[1,2-*b*]pyridin-3-yl)-1H-pyrazol-1-yl]piperidine-1-carboxylate (26 mg, 0.040 mmol) in dichloromethane (0.3 mL) was added HCl (4 M in dioxane, 0.5 mL). The reaction mixture stirred at RT for 1 h. The solution was concentrated in vacuo and diluted with DMSO (1.0 mL) and DMF (1.0 mL). The residue was purified by preparative HPLC reverse phase (C-18), eluting with acetonitrile/water + 0.05% TFA. Fractions containing pure compound were collected, and the free base was liberated using PL-HCO_3 cartridges (Stratospheres, 0.9 mmol) and lyophilized to afford 1-[5-oxo-3-[1-(piperidin-4-yl)-1H-pyrazol-4-yl]-5H-benzo[4,5]cyclohepta[1,2-*b*]pyridin-7-yl]-*N*-(pyridin-2-ylmethyl)methanesulfonamide (5 mg, 0.008 mmol, 21% yield) as a white solid. ^1H NMR (500 MHz, DMSO- d_6) δ 9.27 (d, 1H), 8.61 (s, 1H), 8.59 (d, 1H), 8.47 (m, 1H), 8.23 (s, 1H), 8.15 (d, 1H), 7.80 (m, 4H), 7.41 (m, 2H), 7.34 (d, 1H), 7.26 (m, 1H), 4.64 (s, 2H), 4.42 (m, 1H), 4.23 (d, 1H), 3.28 (m, 2H), 2.93 (m, 2H), 2.18 (m, 2H), 2.03 (m, 2H). MS (ESI) calcd for $\text{C}_{28}\text{H}_{27}\text{N}_7\text{O}_5\text{S}$ $[\text{M} + \text{H}]^+$, 541.2; found, 541.2.

In Vitro Kinase Assays. As described in ref 24, *c*-Met-catalyzed phosphorylation of *N*-biotinylated peptide (EQEDEPEGDYFEWLECONH₂) was measured using a time-resolved fluorescence resonance energy transfer assay. To evaluate kinase selectivity, a single

concentration (1 $\mu\text{mol/L}$) of **11r** and **12** was tested using 221 kinases by Upstate Biotechnology, Inc. (Millipore), which also determined the **11r** IC₅₀ for the kinases for which IC₅₀ values are reported. The **11r** IC₅₀ for Ron, Mer, Flt1, Flt3, Flt4, KDR, PDGFR β , FGFR1, FGFR2, FGFR3, TrkA, and TrkB were determined using time-resolved fluorescence resonance energy transfer assays similar to the *c*-Met kinase assay. For compounds **11a**, **11u**, **11w**, and **13–16**, kinase assays were performed using commercially available ProfilerPro kinase selectivity assay kits from Caliper Life Sciences, Inc. at test concentrations of 0.1 and 1 μM . Compound **5g** was evaluated by Invitrogen, Inc. using a Z'-LYTE kinase assay format or Adapta Universal Kinase Assay at test concentrations of 0.1, 1, and 10 μM . See Supporting Information for tabulated results.

Cellular Assays. As described in ref 24, proliferation and viability of tumor cells was measured using the ViaLight PLUS kit (Cambrex). Analysis of phosphorylation status of *c*-Met, in cells: Tumor cells were treated for 2 h with **11r** or vehicle in RPMI 1640 supplemented with 10% fetal bovine serum and 10 mmol/L HEPES. When called for, the cells were stimulated with HGF during the last 10 min of the 2 h incubation. The cells were lysed with a denaturing or nondenaturing buffer containing phosphatase and protease inhibitors and subjected to Western blot or immunoprecipitation–Western blot analysis.

Tumor Xenograft Model. As described in ref 24, GTL-16 cells were inoculated sc into the flank of female nude CD-1 nu/nu mice. When mean tumor size reached a predetermined range, the mice were randomized and given vehicle or **11r** by po gavage once or twice daily. Tumor volumes were determined using calipers. The percentage increase in the volume of a xenograft tumor on day *n* versus day 0 (the day when dosing of **11r** began) was calculated as (tumor volume on day *n* – tumor volume on day 0)/tumor volume on day 0 \times 100. The mean percentage of tumor growth inhibition in each **11r**-treated group relative to the vehicle-treated group was calculated as (1 – mean percent increase of tumor volume in the **11r**-treated group/mean percent increase of the tumor volume in the vehicle-treated group) \times 100.

Measurement of *c*-Met (Y1349) Phosphorylation in Xenograft Tumors. As described in ref 24, mice bearing GTL-16 tumors were euthanized 1 h after po administration of **11r**. The tumors were excised, snap-frozen, and dispersed using a Qiagen Tissue-Lyser in a nondenaturing lysis buffer containing protease and phosphatase inhibitors. The homogenate was lysed at 4 °C for 1 h, clarified by centrifugation, and then analyzed by quantitative Western blotting for phospho-*c*-Met (Y1349) and total *c*-Met. The pMet (Y1349) signal of each *c*-Met band was normalized with its total *c*-Met signal. To combine or compare data from several gels, the pY1349/total Met ratio for each *c*-Met band was further normalized to the average pY1349/total *c*-Met ratio of the vehicle-treated tumor samples on the same gel.

Time-Dependent Inhibition of CYP3A4. The time-dependent inhibition assay for CYP3A4 was performed in two steps, a preincubation step where the test compound was incubated with human liver microsomes and the secondary incubation period where CYP3A4 substrate, testosterone, was added to the preincubate to measure residual CYP3A4 activity. Wells contained human liver microsomes (42.5 μL , 2.35 mg/mL) which were diluted from a stock (20 mg/mL) in potassium phosphate buffer (50 mM, pH 7.4) such that the final concentration in the 50 μL preincubation was 2 mg/mL. The wells also contained test compound (2.5 μL at 20 times the incubation concentration) in a solvent mixture of DMSO:water:methanol (10:50:40), and the same solvent in the absence of the test compound was used as the control. The final concentrations of the test compound in the preincubations were 1.56, 3.13, 6.25, 12.5, 25, 50, and 100 μM . The preincubation times used were 0, 5, 10, 15, and 20 min. Separate preincubations were used for each preincubation time point. The rack containing the wells was prewarmed for 30 min at 37 °C in an incubator that was gently shaken, and the temperature was maintained at 37 °C for the duration of the incubations. The preincubation period was initiated by the addition of NADPH (5 μL , 10 mM) that had been prewarmed to 37 °C for 10 min. Following the preincubation step, the secondary incubations were initiated by

performing a 10-fold dilution of the preincubate using 450 μL of a prewarmed (37 $^{\circ}\text{C}$) solution of NADPH (1 mM) and testosterone (222 μM) in potassium phosphate (50 mM, pH 7.4). The final concentration of NADPH and testosterone in the 500 μL incubation was 1 mM and 200 μM , respectively. After a 10 min incubation period, each well was quenched with 1 mL of acetonitrile containing the internal standard, cortisone (0.6 $\mu\text{g}/\text{mL}$), and placed on ice. The rack was centrifuged at 3202g for 10 min, and 200 μL of the supernatant was diluted with 100 μL of water, mixed well, and analyzed by LC-MS-MS.

Samples (10 μL) were injected onto a C_{18} column (2.0 mm \times 30 mm, 3 μm particle size) and eluted using water containing 0.1% formic acid as the aqueous mobile phase (A), and acetonitrile containing 0.1% formic acid as the organic phase (B), according to the following gradient table (Table 7):

Table 7

time (min)	flow rate (mL/min)	%A	%B
0.00	0.85	98	2
0.02	0.85	98	2
3.02	0.85	2	98
3.52	0.85	2	98
3.53	0.85	98	2

The eluent from the column was sent to the mass spectrometer and specific multiple reaction monitoring transitions for testosterone metabolite, 6 β -OH testosterone (305 m/z > 269 m/z), and cortisone (361 m/z > 185 m/z) were used for MS/MS detection. Integrated area ratios of the analyte (6 β -OH testosterone) to the internal standard (cortisone) were analyzed by nonlinear regression to calculate K_i and k_{inact} .

Crystallography. Crystals of c-Met were grown essentially as previously described.^{18,25} Crystals were obtained using 15.6 mg/mL enzyme preincubated with a 2-fold molar excess of compound **16** and mixed at a 1:1 ratio with the reservoir solution (150 mM malic acid, 20% PEG 3350, pH 7.0). Diffraction quality crystals were grown by microseeding at 20 $^{\circ}\text{C}$ in sitting drops and stabilized for data collection with reservoir solution plus 20% ethylene glycol. Data were collected at 100 K using a Rigaku FRE+ generator (Rigaku MSC) equipped with a Saturn 944 CCD detector using an X-ray wavelength of 1.54 Å . Oscillation frames of 0.5 $^{\circ}$ were collected over a total rotation range of 240 $^{\circ}$. Data were integrated and reduced with HKL2000. Structures were determined by molecular replacement using the structure of the c-Met kinase domain in complex with K252a (PDB ID: 1R1W) as a starting model for rigid body refinement with REFMAC as implemented in CCP4. The model was rebuilt manually with Coot and completed using iterative rounds of refinement and rebuilding. Structure alignments were performed with SSM and DALI. Figures were prepared with PyMOL.

■ ASSOCIATED CONTENT

Ⓢ Supporting Information

Kinase selectivity profiles of compounds **5g**, **11a**, **11r**, **11u**, **11w**, **12–16**, X-ray statistics for **16**, time course of exposure in the GTL-16 xenograft efficacy and PK/PD experiments, and characterization data for **5b–d**, **11a–f**, **11i–m**, **11p–q**, **11s**, **11u–w**. This material is available free of charge via the Internet at <http://pubs.acs.org>.

Accession Codes

PDB ID 4IWD.

■ AUTHOR INFORMATION

Corresponding Author

*Phone: 617-992-2061. Fax: 617-992-2407. E-mail: alan_northrup@merck.com.

Notes

The authors declare no competing financial interest.

■ ABBREVIATIONS USED

APCI, atmospheric-pressure chemical ionization; Cl_p , plasma clearance; dba, dibenzylideneacetone; EtOAc, ethyl acetate; HATU, *O*-(7-azabenzotriazol-1-yl)-*N,N,N',N'*-tetramethyluronium hexafluorophosphate; MCPBA, *meta*-chloroperoxybenzoic acid; MS/MS, tandem mass spectrometry; MeCN, acetonitrile; RT, room temperature; RuPhos, 2-dicyclohexylphosphino-2',6'-diisopropoxybiphenyl; TDI, time-dependent inhibition of CYP3A4; V_d , volume of distribution; X-Phos, 2-dicyclohexylphosphino-2',4',6'-triisopropylbiphenyl

■ REFERENCES

- (1) For example, see: (a) Mansi, L.; Thierry-Vuillemin, A.; Nguyen, T.; Bazan, F.; Calcagno, F.; Rocquain, J.; Demarchi, M.; Villanueva, C.; Maurina, T.; Pivot, X. Safety profile of new Anticancer Drugs. *Expert Opin. Drug Saf.* **2010**, *9*, 301–317. (b) Mellor, H. R.; Bell, A. R.; Valentin, J.-P.; Roberts, R.R. A. Cardiotoxicity Associated with Targeting Kinase Pathways in Cancer. *Toxicol. Sci.* **2011**, *120*, 14–32. (c) Force, T.; Kolaja, K. L. Cardiotoxicity of Kinase Inhibitors: The Prediction and Translation of Preclinical Models to Clinical Outcomes. *Nature Rev. Drug Discovery* **2011**, *10*, 111–126.
- (2) Zuccotto, F.; Ardini, E.; Casale, E.; Angiolini, M. Through the “Gatekeeper Door”: Exploiting the Active Kinase Conformation. *J. Med. Chem.* **2010**, *53*, 2681–2694.
- (3) Bikker, J. A.; Brooijmans, N.; Wisser, A.; Mansour, T. S. Kinase domain mutations in cancer: implications for small molecule drug design strategies. *J. Med. Chem.* **2009**, *52*, 1493–1509.
- (4) For the discovery and characterization of Nilotinib, see: (a) O'Hare, T.; Walters, D. K.; Deininger, M. W. N.; Druker, B. J. AMN107: Tightening the Grip of Imatinib. *Cancer Cell* **2005**, *7*, 117–119. (b) Weisberg, E.; Manley, P. W.; Breitenstein, W.; Brueggen, J.; Cowan-Jacob, S. W.; Ray, A.; Huntly, B.; Fabbro, D.; Fendrich, G.; Hall-Meyers, E.; Kung, A. L.; Mestan, J.; Daley, G. Q.; Callahan, L.; Catley, L.; Cavazza, C.; Mohammed, A.; Neuberg, D.; Wright, R. D.; Gilliland, D. G.; Griffin, J. D. Characterization of AMN107, a Selective Inhibitor of Native and Mutant Bcr-Abl. *Cancer Cell* **2005**, *7*, 129–141.
- (5) For general references on c-Met and Ron, see (a) Birchmeier, C.; Birchmeier, W.; Gherardi, E.; Vande Woude, G. F. Met, Metastasis, Motility and More. *Nature Rev. Mol. Cell Biol.* **2003**, *4*, 915–925. (b) Benvenuti, S.; Comoglio, P. M. The MET Receptor Tyrosine Kinase in Invasion and Metastasis. *J. Cell. Physiol.* **2007**, *213*, 316–325. (c) Ponzetto, C.; Bardelli, A.; Zhen, Z.; Maina, F.; dalla Zonca, P.; Giordano, S.; Graziani, A.; Panayotou, G.; Comoglio, P. M. A Multifunctional Docking Site Mediates Signaling and Transformation by the Hepatocyte Growth Factor/Scatter Factor Receptor Family. *Cell* **1994**, *77*, 261–271. (d) Accornero, P.; Pavone, L. M.; Baratta, M. The Scatter Factor Signaling Pathways as Therapeutic Associated Target in Cancer Treatment. *Curr. Med. Chem.* **2010**, *17*, 2699–2712.
- (6) For examples of Met mutations or overexpression in human cancer, see (a) Gonzatti-Haces, M.; Seth, A.; Park, M.; Copeland, T.; Oroszlan, S.; Vande Woude, G. F. Characterization of the TPR-MET Oncogene p65 and the MET Proto-oncogene p140 Protein-Tyrosine Kinases. *Proc. Natl. Acad. Sci. U. S. A.* **1988**, *85*, 21–25. (b) Schmidt, L.; Duh, F. M.; Chen, F.; Kishida, T.; Glenn, G.; Choyke, P.; Scherer, S. W.; Zhuang, Z.; Lubensky, I.; Dean, M.; Allikmets, R.; Chidambaram, A.; Bergerheim, U. R.; Feltis, J. T.; Casadevall, C.; Zamarron, A.; Bernues, M.; Richard, S.; Lips, C. J. M.; Walther, M. M.; Tsui, L.-C.; Geil, L.; Orcutt, M. L.; Stackhouse, T.; Lipan, J.; Slife, L.; Brauch, H.; Decker, J.; Niehans, G.; Hughson, M. D.; Moch, H.; Storkel, S.; Lerman, M. I.; Linehan, W. M.; Zbar, B. Germline and Somatic Mutations in the Tyrosine Kinase Domain of the MET Proto-oncogene in Papillary Renal Carcinomas. *Nature Genet.* **1997**, *16*, 68–73. (c) Jeffers, M.; Fiscella, M.; Webb, C. P.; Anver, M.; Koochekpour, S.; Vande Woude, G. F. The Mutationally Activated Met Receptor

- Mediates Motility and Metastasis. *Proc. Natl. Acad. Sci. U. S. A.* **1998**, *95*, 1441–1442. (d) Bean, J.; Brennan, C.; Shih, J.-Y.; Riely, G.; Viale, A.; Wang, L.; Chitale, D.; Motoi, N.; Szoke, J.; Broderick, S.; Balak, M.; Chang, W.-C.; Yu, C.-J.; Gazdar, A.; Pass, H.; Rusch, V.; Gerald, W.; Huang, S.-F.; Yang, P.-C.; Miller, V.; Ladanyi, M.; Yang, C.-H.; Pao, W. MET Amplification Occurs With or Without T790M Mutations in EGFR Mutant Lung Tumors with Acquired Resistance to Gefitinib or Erlotinib. *Proc. Natl. Acad. Sci. U. S. A.* **2007**, *104*, 20932–20937. For examples of Ron mutations or overexpression in human cancer, see (e) Chen, Y. Q.; Zhou, Y. Q.; Angeloni, D.; Kurtz, A. L.; Qiang, X. Z.; Wang, M. H. Overexpression and Activation of the RON Receptor Tyrosine Kinase in a Panel of Human Colorectal Carcinoma Cell Lines. *Exp. Cell Res.* **2000**, *261*, 229–238. (f) Zhou, Y. Q.; He, C.; Chen, Y. Q.; Wang, D.; Wang, M. H. Altered Expression of the RON Receptor Tyrosine Kinase in Primary Human Colorectal Adenocarcinomas: Generation of Different Splicing RON Variants and their Oncogenic Potential. *Oncogene* **2003**, *22*, 186–197. (g) Bardella, C.; Costa, B.; Maggiora, P.; Patane, S.; Olivero, M.; Ranzani, G. N.; De, B. M.; Comoglio, P. M.; Di Renzo, M. F. Truncated RON Tyrosine Kinase Drives Tumor Cell Progression and Abrogates Cell–Cell Adhesion through E-Cadherin Transcriptional Repression. *Cancer Res.* **2004**, *64*, 5154–5161. (h) Zinser, G. M.; Leonis, M. A.; Toney, K.; Pathrose, P.; Thobe, M.; Kader, S. A.; Peace, B. E.; Beauman, S. R.; Collins, M. H.; Waltz, S. E. Mammary-Specific Ron Receptor Overexpression Induces Highly Metastatic Mammary Tumors Associated with Beta-Catenin Activation. *Cancer Res.* **2006**, *66*, 11967–11974.
- (7) Follenzi, A.; Bakovic, S.; Gual, P.; Stella, M. C.; Longati, P.; Comoglio, P. M. Cross-Talk Between the Proto-Oncogenes Met and Ron. *Oncogene* **2000**, *19*, 3041–3049.
- (8) Lee, W.-Y.; Chen, H. H. W.; Chow, N.-H.; Su, W.-C.; Lin, P.-W.; Guo, H.-R. Prognostic Significance of Co-Expression of RON and MET Receptors in Node-Negative Breast Cancer Patients. *Clin. Cancer Res.* **2005**, *11*, 2222–2228.
- (9) Cheng, H.-L.; Liu, H.-S.; Lin, Y.-J.; Chen, H. H.-W.; Hsu, P.-Y.; Chang, T.-Y.; Ho, C.-L.; Tzai, T.-S.; Chow, N.-H. Co-Expression of RON and MET is a Prognostic Indicator for Patients with Transitional-Cell Carcinoma of the Bladder. *Br. J. Cancer* **2005**, *92*, 1906–1914.
- (10) Zou, H. Y.; Li, Q.; Lee, J. H.; Arango, M. E.; McDonnell, S. R.; Yamazaki, S.; Koudriakova, T. B.; Alton, G.; Cui, J. J.; Kung, P.-P.; Nambu, M. D.; Los, G.; Bender, S. L.; Mroczkowski, B.; Christensen, J. G. An Orally Available Small-Molecule Inhibitor of c-Met, PF-2341066, Exhibits Cytoreductive Antitumor Efficacy through Antiproliferative and Antiangiogenic Mechanisms. *Cancer Res.* **2007**, *67*, 4408–4417.
- (11) (a) Qian, F.; Engst, S.; Yamaguchi, K.; Yu, P.; Won, K.-A.; Mock, L.; Lou, T.; Tan, J.; Li, C.; Tam, D.; Lougheed, J.; Yakes, F. M.; Bentzien, F.; Xu, W.; Zaks, T.; Wooster, R.; Greshock, J.; Joly, A. H. Inhibition of Tumor Cell Growth, Invasion, and Metastasis by EXEL-2880 (XL880, GSK1363089), a Novel Inhibitor of HGF and VEGF Receptor Tyrosine Kinases. *Cancer Res.* **2009**, *69*, 8009–8016. (b) See also a recent report of a more selective type II inhibitor: Liu, L.; Norman, M. H.; Lee, M.; Xi, N.; Siegmund, A.; Boezio, A. A.; Booker, S.; Choquette, D.; D'Angelo, N. D.; Germain, J.; Yang, K.; Yang, Y.; Zhang, Y.; Bellon, S. F.; Whittington, D. A.; Harmange, J.-C.; Dominguez, C.; Kim, T. S.; Dussault, I. Structure-Based Design of Novel Class II c-Met Inhibitors: I. Identification of Pyrazolone-Based Derivatives. *J. Med. Chem.* **2012**, *55*, 1858–1867.
- (12) Lu, T.; Alexander, R.; Connors, R. W.; Cummings, M. D.; Galemno, R. A.; Hufnagel, H. R.; Johnson, D. L.; Khalil, E.; Leonard, K. A.; Markotan, T. P.; Maroney, A. C.; Sechler, J. L.; Travins, J. M.; Tuman, R. W. PCT Int. Appl. WO 2007075567, 2007.
- (13) Schadt, O.; Bladt, F.; Blaukat, A.; Dorsch, D.; Friese-Hamim, M.; Fittschen, C.; Graedler, U.; Meyring, M.; Rautenberg, W.; Stieber, F.; Wilm, C. EMD 1214063, An Exquisitely Selective c-Met Kinase Inhibitor in Clinical Phase I. AACR 101st Annual Meeting, Washington, DC, Apr 17–21, 2010; American Association for Cancer Research: Washington, DC, 2010; Poster 5777.
- (14) Cui, J. J.; McTigue, M.; Nambu, M.; Tran-Dubé, M.; Pairish, M.; Shen, H.; Jia, L.; Cheng, H.; Hoffman, J.; Le, P.; Jalaie, M.; Goetz, G. H.; Ryan, K.; Grodsky, N.; Deng, Y.-L.; Parker, M.; Timofeevski, S.; Murray, B. W.; Yamazaki, S.; Aguirre, S.; Li, Q.; Zou, H.; Christensen, J. Discovery of a Novel Class of Exquisitely Selective Mesenchymal–Epithelial Transition Factor (c-MET) Protein Kinase Inhibitors and Identification of the Clinical Candidate 2-(4-(1-(Quinolin-6-ylmethyl)-1H-[1,2,3]triazolo[4,5-b]pyrazin-6-yl)-1H-pyrazol-1-yl)ethanol (PF-04217903) for the Treatment of Cancer. *J. Med. Chem.* **2012**, *55*, 8091–8109.
- (15) Bode, C. M.; Boezio, A. A.; Albrecht, B. K.; Bellon, S. F.; Berry, L.; Broome, M. A.; Choquette, D.; Dussault, I.; Lewis, R. T.; Lin, M.-H.J.; Rex, K.; Whittington, D. A.; Yang, Y.; Harmange, J.-C. Discovery and Optimization of a Potent and Selective Triazolopyridinone Series of c-Met Inhibitors. *Bioorg. Med. Chem. Lett.* **2012**, *22*, 4089–4093.
- (16) Cepero, V.; Sierra, J. R.; Corso, S.; Ghiso, E.; Casorzo, L.; Perera, T.; Comoglio, P. M.; Giordano, S. MET and KRAS Gene Amplification Mediates Acquired Resistance to MET Tyrosine Kinase Inhibitors. *Cancer Res.* **2010**, *70*, 7580–7590.
- (17) Munshi, N.; Jeay, S.; Li, Y.; Chen, C.-R.; France, D. S.; Ashwell, M. A.; Hill, J.; Moussa, M. M.; Leggett, D. S.; Li, C. J. ARQ 197, a Novel and Selective Inhibitor of the Human c-Met Receptor Tyrosine Kinase with Antitumor Activity. *Mol. Cancer Ther.* **2010**, *9*, 1544–1553.
- (18) Katz, J. D.; Jewell, J. P.; Guerin, D. J.; Lim, J.; Dinsmore, C. J.; Deshmukh, S. V.; Pan, B.-S.; Marshall, C. G.; Lu, W.; Altman, M. D.; Dahlberg, W. K.; Davis, L.; Falcone, D.; Gabarda, A. E.; Hang, G.; Hatch, H.; Holmes, R.; Kunii, K.; Lumb, K. J.; Lutterbach, B.; Mathvink, R.; Nazef, N.; Patel, S. B.; Qu, X.; Reilly, J. F.; Rickert, K. W.; Rosenstein, C.; Soisson, S. M.; Spencer, K. B.; Szewczak, A. A.; Walker, D.; Wang, W.; Young, J.; Zeng, Q. Discovery of a 5H-*Benzo*[4,5]cyclohepta[1,2-*b*]pyridin-5-one (MK-2461) Inhibitor of c-Met Kinase for the Treatment of Cancer. *J. Med. Chem.* **2011**, *54*, 4092–4108.
- (19) (a) Kawatsura, M.; Hartwig, J. F. Simple, Highly Active Palladium Catalysts for Ketone and Malonate Arylation: Dissecting the Importance of Chelation and Steric Hindrance. *J. Am. Chem. Soc.* **1999**, *121*, 1473–1478. (b) Fox, J. M.; Huang, X.; Chieffi, A.; Buchwald, S. L. Highly Active and Selective Catalysts for the Formation of α -Aryl Ketones. *J. Am. Chem. Soc.* **2000**, *122*, 1360–1370. (c) Netherton, M. R.; Fu, G. C. Air-Stable Trialkylphosphonium Salts: Simple, Practical, and Versatile Replacements for Air-Sensitive Trialkylphosphines. Applications in Stoichiometric and Catalytic Processes. *Org. Lett.* **2001**, *3*, 4295–4298.
- (20) Grimm, J. B.; Katcher, M. H.; Witter, D. J.; Northrup, A. B. A New Strategy for the Synthesis of Benzylic Sulfonamides: Palladium-Catalyzed Arylation and Sulfonamide Metathesis. *J. Org. Chem.* **2007**, *72*, 8135–8138.
- (21) (a) Mani, S.; Ghalib, M.; Chaudhary, I.; Goel, S. Alterations of Chemotherapeutic Pharmacokinetic Profiles by Drug–Drug Interactions. *Expert Opin. Drug Metab. Toxicol.* **2009**, *5*, 109–130. (b) Mcleod, H. L. Clinically Relevant Drug–Drug Interactions in Oncology. *Br. J. Clin. Pharmacol.* **1998**, *45*, 539–544.
- (22) Kalgutkar, A. S.; Gardner, I.; Obach, R. S.; Shaffer, C. L.; Callegari, E.; Henne, K. R.; Mutlib, A. E.; Dalvie, D. K.; Lee, J. S.; Nakai, Y.; O'Donnell, J. P.; Boer, J.; Harriman, S. P. A Comprehensive Listing of Bioactivation Pathways of Organic Functional Groups. *Curr. Drug Metab.* **2005**, *6*, 161–225 and references therein.
- (23) Significantly, both **5a** and **5g** did not show significant inhibition of CYP3A4 (<10%) at the zero minute time point as potent reversible CYP3A4 inhibitors are not evaluable in this assay format.
- (24) Pan, B.-S.; Chan, G. K. Y.; Chenard, M.; Chi, A.; Davis, L. J.; Deshmukh, S. V.; Gibbs, J. B.; Gil, S.; Hang, G.; Hatch, H.; Jewell, J. P.; Kariv, I.; Katz, J. D.; Kunii, K.; Lu, W.; Lutterbach, B. A.; Paweletz, C. P.; Qu, X.; Reilly, J. F.; Szewczak, A. A.; Zeng, Q.; Kohl, N. E.; Dinsmore, C. J. MK-2461, a Novel Multitargeted Kinase Inhibitor, Preferentially Inhibits the Activated c-Met Receptor. *Cancer Res.* **2010**, *70*, 1524–1533.

(25) Rickert, K. W.; Patel, S. B.; Allison, T. J.; Byrne, N. J.; Darke, P. L.; Ford, R. E.; Guerin, D. J.; Hall, D. L.; Kornienko, M.; Lu, J.; Munshi, S. K.; Reid, J. C.; Shipman, J. M.; Stanton, E. F.; Wilson, K. J.; Young, J. R.; Soisson, S. M.; Lumb, K. J. Structural Basis for Selective Small Molecule Kinase Inhibition of Activated c-Met. *J. Biol. Chem.* **2011**, *286*, 11218–11225.

(26) Lutterbach, B. manuscript in preparation.

(27) Szymonifka, M. J.; Heck, J. V. *Tetrahedron Lett.* **1989**, *30*, 2869–2872.